Double uranium oxo cations derived from uranyl by borane or silane reduction

Bradley E. Cowie,[a] Gary S. Nichol,[a] Jason B. Love*[a] and Polly L. Arnold*[a]

General Details

All manipulations were carried out under a dry, oxygen-free atmosphere of nitrogen using standard Schlenk and glovebox technique. Pyridine was distilled from potassium and stored over 4 Å molecular sieves. THF, toluene and hexanes were degassed and purified by passage through activated alumina towers and stored over 4 Å molecular sieves. All gases were supplied by BOC gases UK. All glassware items, cannulae and Fisherbrand 1.2 μm retention glass microfibre filters were dried in a 150 °C oven overnight before use.

Deuterated solvents, C_6D_6 and d_5-pyridine, were boiled over potassium, freeze−pump−thaw degassed and vacuum-transferred prior to use. ^{1}H, $^{13}C\{^{1}H\}$, ^{11}B and ^{29}Si NMR spectra were recorded on Bruker AVA400, AVA500, or PRO500 spectrometers at 298 K. Chemical shifts are reported in parts per million, δ. All ^{1}H NMR and $^{13}C\{^{1}H\}$ NMR spectra were referenced relative to $SiMe_4$ through a resonance of the employed deuterated solvent or proteo impurity of the solvent; C_6D_6 (7.16 ppm) and d_5-pyridine (8.74, 7.58, 7.22 ppm) for ^{1}H NMR; C_6D_6 (128.0 ppm) and d_5-pyridine (150.35, 135.91, 123.87 ppm) for $^{13}C\{^{1}H\}$ NMR. ^{1}H NMR data for complexes **2**-**4** are reported on isolated samples, whereas ^{1}H NMR data for **5** is reported on an *in-situ* generated sample due the poor solubility of this complex once isolated. ^{11}B and ^{29}Si NMR spectra were referenced using an external standard of $BF_3(OEt_2)$ (0.0 ppm) and $SiMe_4$ (0.0 ppm), respectively. Infrared spectra were recorded on a Perkin Elmer Spectrum 65 FT-IR spectrometer as nujol mulls between NaCl disks. Elemental analyses were carried out at Pascher Labor, Germany or at the London Metropolitan University.

Single crystal X-ray diffraction data for **2·2toluene** and **3·THF** was collected on a Bruker SMART APEXII diffractometer fitted with a CCD area detector using MoKα radiation (λ = 0.71073 Å) at 150(2) K. Single crystal X-ray data for **4·5.5THF** was collected using an Oxford Diffraction Supernova instrument at 120(2) K, fitted with a CCD area detector using MoKα radiation. Single crystal X-ray diffraction data for **5·py** and **5·2THF** were collected using an Excalibur Eos diffractometer, fitted with a CCD area detector and using MoKα radiation; data for **5·py** was collected at 120(2) K, whereas data for **5·2THF** was collected at 173(2) K.

$HN(SiMe_3)_2$, B_2pin_2, B_2cat_2, HBpin, Ph_2SiH_2 and $BF_3{\cdot}OEt_2$ were purchased from Sigma-Aldrich; $HN(SiMe_3)_2$ was used as was, B_2pin_2 and B_2cat_2 were stored in the glove box prior to use, and Ph_2SiH_2, HBpin and $BF_3{\cdot}OEt_2$ were distilled and stored in the glove box prior to use. HBcat was purchased from Alfa Aesar and stored in the glove box freezer prior to use. $LiN(SiMe_3)_2$ was purchased from Sigma Aldrich and sublimed at 110 °C at $1{\times}10^{-4}$ Torr. KH (suspension in oil) was purchased from Fischer Scientific, washed with hexanes to remove the oil, and solid KH was stored in the glove box. $KN(SiMe_3)_2$,[1] $[UO_2\{N(SiMe_3)_2\}_2(THF)_2]$[2] and the H_4L^A ligand[3] were prepared according to the literature procedures. The synthesis of $[\{UO_2(py)\}_2(L^A)]$ (**1**) has been previously reported,[4] however an improved procedure is provided below.

Syntheses

Improved Synthesis of [{UO_2(py)}$_2$(L^A)] (**1**)

[UO_2{$N(SiMe_3)_2$}$_2$($THF)_2$] (3.04 g, 4.13 mmol) and H_4L^A (1.43 g, 1.65 mmol) were combined in a 200 mL ampoule fitted with a Young's tap, to which pyridine (100 mL) was added via cannula. The reaction mixture was stirred for 3 days at room temperature. The reaction mixture was then cannulated into a 200 mL Schlenk flask and evaporated to dryness under reduced pressure. Hexanes (~100 mL) were added to the dark brown, oily residue and the resulting slurry was sonicated and filtered. The remaining pale brown-green solid was washed with hexanes (2×100 mL) and filtered, then dried under reduced pressure. Yield = 2.05 g (80 %).

[{(py)pinBO}UOU{OBpin(py)}(L^A)] (**2**)

(a) From B_2pin_2: Complex **1** (356 mg, 0.229 mmol) and B_2pin_2 (116 mg, 0.458 mmol) were combined in a 200 mL ampoule fitted with a Young's tap, to which pyridine (50 mL) was added via cannula. The reaction mixture was stirred for 6 hours under a static argon atmosphere at 80 °C. The reaction mixture was then cannulated into a 200 mL Schlenk flask and evaporated to dryness under reduced pressure. Hexanes (~50 mL) were added to the dark brown, oily residue by cannula and the resulting slurry was sonicated and filtered. The remaining light brown solid was washed with hexanes (2×50 mL) and filtered; the hexanes washings took on a yellow colour during each filtration, indicating that the desired **2** was hexanes-soluble. The remaining solid was then dried under reduced pressure. Yield = 193 mg (47 %). X-ray quality crystals of **2·2toluene** were grown by slow evaporation of a toluene solution of **2** under an inert atmosphere. **Elemental Analysis:** Found: C, 53.32; H, 4.83; N, 7.55. Calc. for $C_{80}H_{82}B_2N_{10}O_7U_2$: C, 53.58; H, 4.61; N, 7.81 %. **IR (Nujol Mull, ν_{max}/cm^{-1}):** 1599s, 1557s, 1454s, 1409s, 1378s, 1313m, 1282s, 1268s, 1252s, 1214m, 1116m, 1150s, 1105m, 1086m, 1056s, 1038m, 1014s, 919w, 905w, 877s, 852m, 786w, 766w, 752m, 742m, 720m, 704m, 696m, 679w, 650w, 626w, 605w, 566s (asym. OUO), 531w, 519w. **δ^1H NMR (500 MHz; d_5-pyridine; 298 K; $SiMe_4$):** 28.64 (12H, s, $BO_2C_2(CH_3)_4$), 25.34 (2H, s, L^A-CH_{aryl}), 21.06 (2H, s, L^A-CH_{aryl}), 16.69 (2H, br s), 10.40 (2H, s, L^A-CH_{aryl}), 9.43 (12H, s, $BO_2C_2(CH_3)_4$), 8.83 (2H, s), 6.38 (2H, s), 5.30 (2H, br s), 3.85 (2H, s, L^A-CH_{aryl}), 2.41 (3H, br s), 2.22 (3H, s), –0.32 (2H, br s), –2.62 (2H, s, L^A-CH_{aryl}), –2.66 (2H, s), –4.17 (2H, br s), –6.01 (2H, s, L^A-CH_{aryl}), –6.36 (2H, s), –12.56 (2H, s), –16.73 (2H, s), –17.19 (2H, br s), –20.40 (2H, s), –41.90 (2H, br s). **δ^{13}C{^{1}H} NMR (126 MHz; d_5-pyridine; 298 K; $SiMe_4$):** 221.6 (s), 177.7 (s), 176.4 (s), 151.4 (s), 141.2 (s), 138.5 (s), 129.9 (s), 129.1 (s), 127.7 (br s), 126.2 (s), 122.6 (s), 118.9 (s), 117.3 (s), 115.9 (s), 111.8 (s), 105.6 (br s), 103.5 (s), 101.7 (s), 101.4 (s), 100.2 (s), 98.2 (br s), 93.9 (br s), 91.3 (s), 82.0 (s), 81.8 (br s), 68.7 (br s), 60.5 (br s), 59.7 (br s), 51.8 (br s), 50.1 (br s), 45.2 (br s), 37.2 (s), 32.2 (s), 31.9 (s), 29.8 (br s), 25.6 (s), 23.3 (s), 21.8 (s), 15.5 (s), 14.7 (s), 11.7 (br s), 7.9 (s), –1.1 (br s), –10.4 (br s). **δ^{11}B NMR (161 MHz; d_5-pyridine; 298 K; $BF_3(OEt_2)$):** 475 (br s), 221 (br s). **δ^{11}B NMR (161 MHz; C_6D_6; 298 K; $BF_3(OEt_2)$):** 471 (br s), 213 (br s).

(b) From HBpin: Complex **1** (17.5 mg, 1.13×10^{-2} mmol) and HBpin (14.5 mg, 0.113 mmol) were combined in a J-Young NMR tube, to which d_5-pyridine (~0.6 mL) was added. The

reaction mixture was heated for 3 days at 125 °C, and the successful synthesis of **2** was verified by ^{1}H and ^{11}B NMR spectroscopy.

[(py){(py)catBO}UOU{OBcat(py)}(L^A)] (**3**)

***In-Situ* Generation:** Complex **1** (28.9 mg, 1.86×10^{-2} mmol) and B_2cat_2 (13.3 mg, 5.59×10^{-2} mmol) were combined in J-Young NMR tube, to which d_5-pyridine (~0.6 mL) was added. The reaction mixture was heated for 6 hours at 80 °C without agitation. **Note:** Physical mixing of the solution of **1** and B_2cat_2 during the reaction period resulted in the formation of a mixture of **3**, **4** and unreacted **1**. X-ray quality crystals of **3·THF** were obtained by vapour diffusion of hexanes into a solution of **3** in THF at room temperature. Yield = ~10 mg. **IR (Nujol Mull, ν_{max}/cm^{-1}):** 1717w, 1591m, 1552m, 1536m, 1482s, 1459s, 1378s, 1354m, 1337m, 1311m, 1299m, 1282m, 1236m, 1219m, 1170m, 1149m, 1098m, 1054s, 1007m, 972m, 963m, 907m, 873m, 865m, 839m, 827m, 804w, 786w, 735s, 722s, 702w, 681w, 664w, 656w, 635w, 623w, 605w, 595w, 580m (asym. OUO; tentative), 562w, 531m (asym. OUO; tentative). **δ^1H NMR (500 MHz; d_5-pyridine; 298 K; $SiMe_4$):** 63.01 (1H, br s), 27.71 (3H, s), 17.90 (4H, s), 12.90 (3H, s), 5.52-5.11 (12H, m), –0.39 (4H, br s), –2.04 (4H, s), –3.63, –3.77 (4H, 2×br s), –6.75 (3H, s), –7.37 (3H, s), –9.67 (4H, s), –10.71 (4H, s), –14.87 (4H, s), –17.07 (2H, s), –24.12 (4H, s), –26.04 (2H, br s). **δ^{13}C NMR (126 MHz; d_5-pyridine; 298 K; $SiMe_4$):** 217.8 (s), 158.9 (s), 154.2 (s), 152.9 (s), 152.7 (s), 152.6 (s), 147.7 (br s), 138.9 (s), 137.8 (br s), 137.5 (br s), 129.1 (s), 126.2 (s), 122.5 (2×s), 121.7 (s), 120.9 (s), 120.7 (s), 120.6 (s), 120.5 (s), 120.0 (s), 119.5 (s), 118.5 (s), 116.1 (s), 114.5 (s), 112.1 (s), 111.2 (s), 111.1 (s), 111.0 (s), 110.9 (s), 110.5 (s), 109.3 (2×s), 108.9 (s), 107.9 (s), 106.1 (s), 105.2 (s), 103.5 (s), 102.4 (s), 99.6 (s), 98.4 (s), 88.3 (s), 84.6 (br s), 73.2 (br s), 70.6 (s), 68.3 (s), 63.4 (br s), 57.1 (br s), 45.6 (s), 45.6 (s), 32.1 (s), 30.1 (s), 27.6 (s), 26.2 (s), 25.3 (s), 23.3 (s), 21.8 (s), 21.1 (br s), 17.7 (s), 15.7 (br s), 14.7 (s), –0.64 (br s), –3.9 (br s), –29.9 (br s). **δ^{11}B NMR (161 MHz; d_5-pyridine; 298 K; $BF_3(OEt_2)$):** δ 496 (br s), 126 (br s). **δ^{11}B NMR (161 MHz; C_6D_6; 298 K; $BF_3(OEt_2)$):** δ 493 (br s), 130 (br s).

[(py)UOU(μ-$O_2C_6H_4$)(py)(L^A)] (**4**)

(a) From B_2cat_2: Complex **1** (294 mg, 0.189 mmol) and B_2cat_2 (135 mg, 0.567 mmol) were combined in a 200 mL ampoule fitted with a Young's tap, to which pyridine (50 mL) was added via cannula. The reaction mixture was stirred for 3 days under a static argon atmosphere at 105 °C, after which the reaction mixture was cannulated into a 200 mL Schlenk flask and evaporated to dryness under reduced pressure. Toluene (~30 mL) was added to the dark brown, oily residue by cannula and the resulting slurry was sonicated and filtered. The remaining light brown solid was washed with toluene (2×30 mL) and filtered. The remaining solid was then dried under reduced pressure. Yield = 235 mg (77 %). X-ray quality crystals of **4·4THF·hexanes** were grown by vapour diffusion of hexanes into a THF solution of **4** at room temperature. **Elemental Analysis:** Found: C, 54.04; H, 4.06; N, 8.74. Calc. for $C_{74}H_{62}N_{10}O_3U_2$: C, 55.02; H, 3.87; N, 8.67 %. **IR (Nujol Mull, ν_{max}/cm^{-1}):** 1594s, 1558s, 1482s, 1457s, 1378s, 1353w, 1317w, 1286s, 1275s, 1265s, 1251s, 1238s, 1213m, 1172w, 1151w, 1102w, 1087w, 1056m, 1046m, 1036m, 1016w, 1006w, 979w, 967w, 959w, 905w, 893w, 878w, 866w, 832m, 791w, 760m, 754m, 737s, 722m, 698m, 658w, 628w, 617m, 607w, 590w, 581w, 565w, 556w,

521w. **δ[1]H NMR (500 MHz; d_5-pyridine; 298 K; $SiMe_4$):** 70.58 (2H, s), 46.59 (2H, br s), 41.30 (2H, s), 27.53 (4H, s), 26.64 (4H, s), 20.88 (2H, s), 20.55 (6H, s), 15.79 (4H, s), 13.58 (6H, s), 8.25 (4H, br s), 6.94 (4H, s), 3.01 (4H, s), –18.91 (2H, br s), –24.57 (4H, s), –60.36 (2H, s). **δ[13]C{[1]H} NMR (126 MHz; d_5-pyridine; 298 K; $SiMe_4$):** 256.4 (br s), 254.4 (br s), 187.0 (s), 185.8 (s), 177.7 (br s), 176.5 (br s), 156.9 (s), 154.0 (s), 153.0 (s), 152.7 (s), 151.6 (s), 151.4 (s), 145.9 (s), 145.5 (s), 145.3 (s), 145.1 (s), 143.8 (br s), 137.6 (s), 137.0 (br s), 127.6 (s), 124.6 (s), 122.2 (s), 121.6 (s), 120.6 (s), 119.6 (s), 118.6 (s), 111.2 (s), 110.2 (s), 109.4 (s), 102.3 (br s), 99.4 (br s), 64.8 (s), 56.6 (t, *J* 120 Hz), 40.2 (s), 32.6 (br s), 27.4 (s), 23.3 (s), 14.7 (s), 2.4 (s), –5.8 (br s), –6.9 (br s).

(b) From HBcat: Complex **1** (20.1 mg, 1.29×10^{-2} mmol) and HBcat (15.6 mg, 0.130 mmol) were combined in a J-Young NMR tube, to which d_5-pyridine (~0.6 mL) was added. The reaction mixture was heated for 7 days at 105 °C, and the successful synthesis of **4** was verified by ^{1}H NMR spectroscopy (500 MHz; d_5-pyridine; 298 K; $SiMe_4$).

[{(py)HPh_2SiO}UOU{$OSiPh_2H$(py)}(L^A)] (5)

Complex **1** (306 mg, 0.197 mmol), Ph_2SiH_2 (544 mg, 2.95 mmol) and $KN(SiMe_3)_2$ (10.0 mg, 5.01×10^{-2} mmol) were combined in a 200 mL ampoule fitted with a Young's tap, to which pyridine (100 mL) was added via cannula. The reaction mixture was stirred for 48 hours under a static argon atmosphere at 125 °C. The reaction mixture was then cannulated into a 200 mL Schlenk flask and evaporated to dryness under reduced pressure, yielding a dark brown oil. Hexanes (~40 mL) were added and the resulting slurry was sonicated and filtered. The remaining light brown solid was washed with hexanes (2×40 mL) and filtered. The remaining solid was then dried under reduced pressure. Yield = 234 mg (62 %). X-ray quality crystals of **5·THF** were grown by vapour diffusion of hexanes into a THF solution of **5** at room temperature, and X-ray quality crystals of **5·py** were grown from a concentrated solution of **5** in pyridine at room temperature. **Elemental Analysis:** Found: C, 58.05; H, 4.32; N, 7.14. Calc. for $C_{92}H_{80}N_{10}O_3Si_2U_2$: C, 57.98; H, 4.23; N, 7.35 %. **IR (Nujol Mull, ν_{max}/cm^{-1}):** 2126w, 1706w, 1588s, 1552m, 1458s, 1376m, 1296w, 1274m, 1114m, 1068m, 1052m, 1016m, 922m, 870m, 840m, 816m, 750w, 736m, 700m, 658w, 630w, 598w, 569w. **δ[1]H NMR (500 MHz; d_5-pyridine; 298 K; $SiMe_4$):** 63.96 (8H, s), 24.82 (12H, s), 20.51 (6H, s), –7.06 (4H, s), –7.45 (5H, s), –9.12 (2H, br s), –11.10 (3H, s), –16.25 (6H, s), –20.76 (4H, br s), –31.91 (8H, s), –41.28 (3H, br s).

From Other MX Salts, $BF_3(OEt_2)$ and $B(C_6F_5)_3$

(a) From $LiN(SiMe_3)_2$: Complex **1** (26.9 mg, 1.73×10^{-2} mmol), Ph_2SiH_2 (47.8 mg, 0.259 mmol) and $LiN(SiMe_3)_2$ (0.7 mg, 4.18×10^{-3} mmol) were combined in a J-Young NMR tube, to which d_5-pyridine (~0.6 mL) was added. The reaction mixture was heated overnight at 125 °C and analysed by ^{1}H NMR spectroscopy (500 MHz; d_5-pyridine; 298 K; $SiMe_4$). The resulting ^{1}H NMR spectrum appeared the same as that of **5**.

(b) From KO^{t}Bu: Complex **1** (27.3 mg, 1.76×10^{-2} mmol), Ph_2SiH_2 (48.5 mg, 0.263 mmol) and KO^{t}Bu (0.5 mg, 4.46×10^{-3} mmol) were combined in a J-Young NMR tube, to which d_5-pyridine (~0.6 mL) was added. The reaction mixture was heated overnight at 125 °C and

analysed by ^{1}H NMR spectroscopy (500 MHz; d_5-pyridine; 298 K; $SiMe_4$). The resulting ^{1}H NMR spectrum appeared the same as that of **5**.

(c) Attempted Synthesis from $BF_3(OEt_2)$: Complex **1** (26.1 mg, 1.68×10^{-2} mmol), Ph_2SiH_2 (46.4 mg, 0.252 mmol) and $BF_3(OEt_2)$ (0.6 mg, 4.23×10^{-3} mmol) were combined in a J-Young NMR tube, to which d_5-pyridine (~0.6 mL) was added. The reaction mixture was heated overnight at 125 °C and analysed by ^{1}H NMR spectroscopy (500 MHz; d_5-pyridine; 298 K; $SiMe_4$). The resulting NMR spectrum appeared the same as that of **1**, indicating that no reaction had occurred

(d) Attempted Synthesis from $B(C_6F_5)_3$ in pyridine: Complex **1** (23.6 mg, 1.52×10^{-2} mmol), Ph_2SiH_2 (42.0 mg, 0.228 mmol) and $B(C_6F_5)_3$ (1.9 mg, 3.71×10^{-3} mmol) were combined in a J-Young NMR tube, to which d_5-pyridine (~0.6 mL) was added. The reaction mixture was heated overnight at 125 °C and analysed by ^{1}H NMR spectroscopy (500 MHz; d_5-pyridine; 298 K; $SiMe_4$). The resulting NMR spectrum appeared the same as that of **1**, indicating that no reaction had occurred.

(e) Attempted Synthesis from $B(C_6F_5)_3$ in iodobenzene/C_6D_6 (anticipated high-boiling, inert, non-coordinating solvent): Complex **1** (22.1 mg, 1.42×10^{-2} mmol), Ph_2SiH_2 (39.3 mg, 0.213 mmol) and $B(C_6F_5)_3$ (1.8 mg, 3.52×10^{-3} mmol) were combined in a J-Young NMR tube, to which iodobenzene (~0.5 mL) and C_6D_6 (~0.1 mL) were added. The reaction mixture (a barely-soluble suspension) was heated overnight at 125 °C and analysed by ^{1}H NMR spectroscopy (500 MHz; d_5-pyridine; 298 K; $SiMe_4$). The resulting ^{1}H NMR spectrum indicated that no reaction had occurred.

pin(py)BOBpin/pin(py)BOB(py)pin

B_2pin_2 (22 mg, 8.7×10^{-2} mmol) and Me_3NO (6.6 mg, 8.8×10^{-2} mmol) were combined in a J-Young NMR tube, to which d_5-pyridine (~0.6 mL) was added. The reaction mixture was allowed to sit at room temperature for 30 minutes and then analysed by ^{1}H and ^{11}B NMR spectroscopy. **δ^{1}H NMR (500 MHz; d_5-pyridine; 298 K; $SiMe_4$):** 1.20 (24H, s, $BO_2C_2(CH_3)_4$ × 2). **δ^{11}B NMR (161 MHz; d_5-pyridine; 298 K; $BF_3(OEt_2)$):** 23 (s, *B*$O_2C_2(CH_3)_4$), 16 (s, *B*(py)$O_2C_2(CH_3)_4$).

cat(py)BOBcat/cat(py)BOB(py)(cat)

B_2cat_2 (24 mg, 0.10 mmol) and Me_3NO (7.6 mg, 0.10 mmol) were combined in a J-Young NMR tube, to which d_5-pyridine (~0.6 mL) was added. The reaction mixture was allowed to stand at room temperature overnight and then analysed by ^{1}H and ^{11}B NMR spectroscopy. **δ^{1}H NMR (500 MHz; d_5-pyridine; 298 K; $SiMe_4$):** 7.02 (minor product (~25 %), dd, $^{3}J_{H,H}$ 6, 3 Hz, B*cat*), 6.91 (4H, dd, $^{3}J_{H,H}$ 6, 3 Hz, B(py)*cat*), 6.80 (minor product (~25 %), dd, $^{3}J_{H,H}$ 6, 3 Hz, B*cat*), 6.78 (4H, dd, $^{3}J_{H,H}$ 6, 3 Hz, B(py)*cat*). **δ^{11}B NMR (161 MHz; d_5-pyridine; 298 K; $BF_3(OEt_2)$):** 15 (s, *B*cat), 9 (s, *B*(py)cat).

Crystallographic Details

General X-ray Experimental Details

The molecular structures of **2·2toluene**, **3·THF**, **4·5.5THF**, **5·py** and **5·2THF** were solved using SHELXT[5] and least-square refined using SHELXL[6] in Olex2.[7] Hydrogen atoms were treated by constrained refinement, except for H(80) and H(80') in **5·py** and **5·2THF**, which were located in the difference map.

The axially coordinated OBpin ligand in **2·2toluene** (O(1), B(1), O(4), O(5), C(69), C(70), C(71), C(72), C(73), C(74)) was positionally/rotationally disordered over two positions, so was split into two parts and refined with an occupancy ratio of 0.79:0.21. The minor component is rotated nearly 90 degrees to the major component, and anisotropic refinement of the thermal parameters of the minor component resulted in unstable refinement. As a result, they were refined isotropically. The thermal parameters of both parts were also restrained through the use of the RIGU command, and the thermal and positional parameters of B(1) and B(1A) were refined to be equal to one another through the use of the EADP and EXYZ commands, respectively. Second, C(8) was positionally disordered over two positions, so was split into two parts and refined anisotropically with an occupancy ratio of 0.67:0.33. The thermal parameters of C(8) and C(8A) were refined to be similar to one another through the use of the SIMU command. Finally, both molecules of toluene within the lattice were positionally disordered over two positions. Both were split into two parts and refined anisotropically in a 0.54:0.44 (C(100)-C(106):C(110)-C(116); C(120)-C(126):C(130)-C(136)) ratio. Furthermore, the aryl C- and H-atoms of toluene C(130)-C(135) were restrained to lie in a common plane through the use of the FLAT command, the thermal parameters of the toluene molecules C(120)-C(126) and C(130)-C(136) were restrained using the RIGU command, and the C(100)–C(106), C(110)–C(116) and C(120)–C(126) bond lengths were fixed at 1.52 Å using the DFIX command. In terms of **3·THF**, we attempted to split the thermal parameters of C(92) of the lattice THF molecule into two parts to model the positional disorder, however this resulted in unstable refinement of the THF molecule. As a result, the thermal parameters of the THF carbon atoms were restrained to be similar to one another using the SIMU command. With respect to **4·5.5THF**, in the solid-state it has crystallographically imposed mirror symmetry, with the central oxygen atom of the complex (O(3)) and the oxygen atom of lattice THF (O(30)) positioned on the mirror plane. C(8) was positionally disordered over two positions, so it's thermal parameters were split into two parts with an occupancy set to 0.5 and refined anisotropically. As a result, H(8B) was positionally disordered, so it's thermal parameters were also split into two parts and refined with an occupancy of 0.5. Furthermore, 2.5 molecules of THF were SQUEEZED from the lattice of **4·5.5THF** through the use of the SQUEEZE routine[8] due to unresolvable disorder. Two of the lattice THF molecules (O(10), C(100), C(101), C(102), C(103), and O(20), C(200), C(201), C(202), C(203)) were disordered, so the C–O bond lengths in each molecule of THF were restrained using the SADI command, and the overall geometry of both THF molecules were constrained to have a similar geometry to the third molecule of lattice THF (O(30), C(300), C(300'), C(301), C(301')) through the use of the SAME command. The THF lattice solvent in **5·2THF** was positionally disordered over two positions, so it's thermal parameters were split into two parts and refined anisotropically in a 0.31:0.69 ratio. In addition, the thermal parameters of the THF molecule were restrained to be similar to one another through the use of the SIMU and DELU commands. This complex also possesses crystallographically imposed two-fold symmetry, with the central oxygen O(3) located on the two-fold axis. Lastly, the pyridine lattice solvent in **5·py** was positionally disordered, so it's occupancy was set to 0.5 and refined over two

positions. This complex possesses crystallographically imposed two-fold symmetry, with the central oxygen O(3) positioned on the two-fold axis.

Standard X-Ray Details for Each Complex

Table S1. Crystallographic data summary for complexes **2·2toluene**, **3·THF** and **4·5.5THF**. CCDC codes 1812761-1812765.

Complex	[{(py)pinBO}UOU{OBpin(py)}(L^A)] (**2·2toluene**)	[(py){(py)catBO}UOU{OBcat(py)}(L^A)] (**3·THF**)	[(py)UOU(μ-$C_6H_4O_2$)(py)(L^A)] (**4·5.5THF**)
Name in cif	2.2toluene	3.THF	4.5.5THF
Local code	po17021	po17028	po17018_refinalized_sq
Chemical formula	$C_{80}H_{82}B_2N_{10}O_7U_2 \cdot 2(C_7H_8)$	$C_{85}H_{71}B_2N_{11}O_7U_2$, C_4H_8O	$C_{74}H_{62}N_{10}O_3U_2 \cdot 5.5(C_4H_8O)$
M_r	1977.50	1928.36	2011.9573
Crystal system, space group	Triclinic, *P*–1	Triclinic, *P*–1	Monoclinic, $P2_1/m$
Temperature (K)	150(2)	150(2)	120(2)
a, *b*, *c* (Å)	14.7593(5), 15.6981(6), 20.1394(7)	14.8167(3), 15.0681(3), 18.9308(4)	14.0794(3), 21.2409(5), 14.5407(4)
α, β, γ (°)	74.615(2), 87.841(2), 69.604(2)	68.593(1), 79.072(1), 86.228(1)	90, 105.116(3), 90
V (Å^3)	4209.1(3)	3863.52	4198.1(2)
Z	2	2	2
Radiation type	Mo Kα	Mo Kα	Mo Kα
μ (mm^{-1})	3.905	4.253	3.908
Crystal size (mm)	0.820×0.440×0.200	0.210×0.160×0.160	0.331×0.240×0.105
Diffractometer	Bruker SMART APEXII diffractometer	Bruker SMART APEXII diffractometer	SuperNova, Dual, Cu at zero, Atlas
Absorption correction	SADABS 2014/5	SADABS 2014/5	Gaussian *CrysAlis PRO* 1.171.38.42b (Rigaku Oxford Diffraction, 2015) Numerical absorption correction based on gaussian integration over a multifaceted crystal model Empirical absorption correction using spherical harmonics, implemented in SCALE3 ABSPACK scaling algorithm.
T_{min}, T_{max}	0.1950, 0.6435	0.469, 0.549	0.3579, 0.6953
θ_{min}, θ_{max}	1.758, 28.316	3.01, 28.02	3.05, 26.37
No. of measured, independent and observed [$I > 2\sigma(I)$] reflections	192088, 20508, 17854	88345, 18474, 14137	86045, 8803, 7308
R_{int}	0.0284	0.0501	0.0703
$R[F^2 > 2\sigma(F^2)]$, $wR(F^2)$, *S*	0.0247, 0.0569, 1.134	0.0298, 0.0586, 1.013	0.0432, 0.0978, 1.056
No. of reflections	20508	18474	8803
No. of parameters	1145	1009	517
No. of restraints	253	18	103
$\Delta\rho_{max}$, $\Delta\rho_{min}$ (e Å^{-3})	2.23, –1.52	1.10, –1.07	2.18, –1.12

Table S2. Crystallographic data summary for complexes **5·py** and **5·2THF**.

Complex	[{(py)HPh$_2$SiO}UOU{OSiPh$_2$H(py)}(L^A)] (**5·py**)	[{(THF)HPh$_2$SiO}UOU{OSiPh$_2$H(THF)}(L^A)] (**5·2THF**)
Name in cif	5py.py	5THF.2THF
Local code	P17134a_mono_80_2	P16085_mono_c
Chemical formula	$C_{92}H_{80}N_{10}O_3Si_2U_2 \cdot C_5H_5N$	$C_{90}H_{86}N_8O_5Si_2U_2 \cdot 2(C_4H_8O)$
M_r	1985.00	2036.12
Crystal system, space group	Monoclinic, *C*2/*c*	Monoclinic, *C*2/*c*
Temperature (K)	120(2)	173(2)
a, *b*, *c* (Å)	23.8381(5), 17.7807(2), 21.4711(4)	22.5124(2), 19.8405(2), 20.1410(2)
α, β, γ (°)	90, 114.099(2), 90	90, 110.283(1), 90
V (Å^3)	8307.5(3)	8438.3(1)
Z	4	4
Radiation type	Mo Kα	Mo Kα
μ (mm^{-1})	3.982	3.925
Crystal size (mm)	0.198×0.085×0.062	0.35×0.23×0.08
Diffractometer	Xcalibur, Eos	Xcalibur, Eos
Absorption correction	Analytical *CrysAlis PRO* 1.171.38.42b (Rigaku Oxford Diffraction, 2015) Analytical numeric absorption correction using a multifaceted crystal model based on expressions derived by R.C. Clark & J.S. Reid. (Clark, R. C. & Reid, J. S. (1995). Acta Cryst. A51, 887-897) Empirical absorption correction using spherical harmonics, implemented in SCALE3 ABSPACK scaling algorithm.	Analytical *CrysAlis PRO* 1.171.38.42b (Rigaku Oxford Diffraction, 2015) Analytical numeric absorption correction using a multifaceted crystal model based on expressions derived by R.C. Clark & J.S. Reid. (Clark, R. C. & Reid, J. S. (1995). Acta Cryst. A51, 887-897) Empirical absorption correction using spherical harmonics, implemented in SCALE3 ABSPACK scaling algorithm.
T_{min}, T_{max}	0.850, 0.947	0.3404, 0.7442
θ_{min}, θ_{max}	2.96, 26.37	3.0660, 28.693
No. of measured, independent and observed [$I > 2\sigma(I)$] reflections	125163, 8502, 7300	88911, 8628, 7290
R_{int}	0.0977	0.0598
$R[F^2 > 2\sigma(F^2)]$, $wR(F^2)$, S	0.0299, 0.0565, 1.059	0.0267, 0.0573, 1.040
No. of reflections	8502	8628
No. of parameters	540	586
No. of restraints	0	132
$\Delta\rho_{max}$, $\Delta\rho_{min}$ (e Å^{-3})	0.90, –0.64	1.21, –0.50

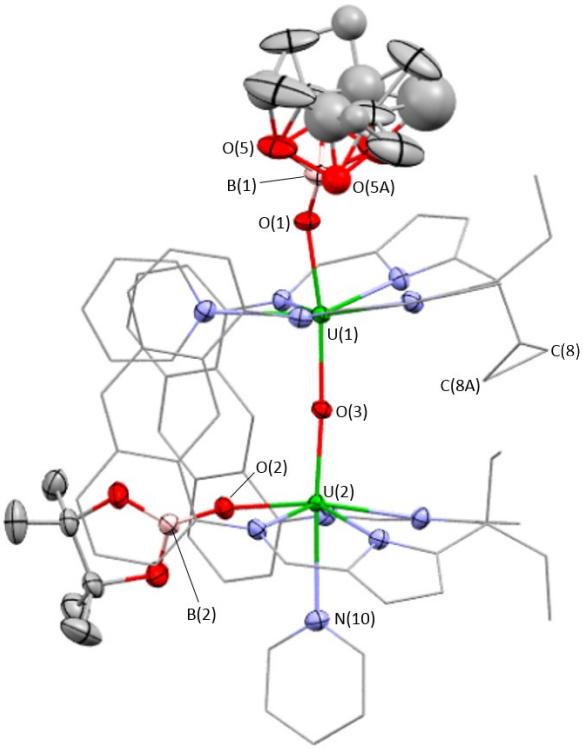

Figure S1. Solid-state structure of **2·2toluene** with thermal ellipsoids drawn at 50% probability, carbon atoms of the L^A ligand and U-coordinated solvent drawn wireframe, and hydrogen atoms and lattice solvent omitted for clarity. C(8) is positionally disordered over two positions, so it's thermal parameters are split into two parts (labelled as C(8) and C(8A) above). The OBpin ligand coordinated in the axial position is also positionally/rotationally disordered, so it's thermal parameters are split into two parts (0.79:0.21 ratio); the minor component was refined isotropically. Key bond lengths [Å] and angles [°]: U(1)–O(1), 2.161(2); U(2)–O(2), 2.172(2); U(1)–O(3), 2.139(2); U(2)–O(3), 2.112(2); O(1)–B(1), 1.334(4); O(2)–B(2), 1.341(4); U(1)–N_{avg}, 2.535(5); U(2)–N_{avg}, 2.559(5); O(1)–U(1)–O(3), 169.05(8); O(2)–U(2)–O(3), 96.51(7); U(1)–O(3)–U(2), 176.2(1); B(1)–O(1)–U(1), 145.7(2); B(2)–O(2)–U(2), 166.9(2).

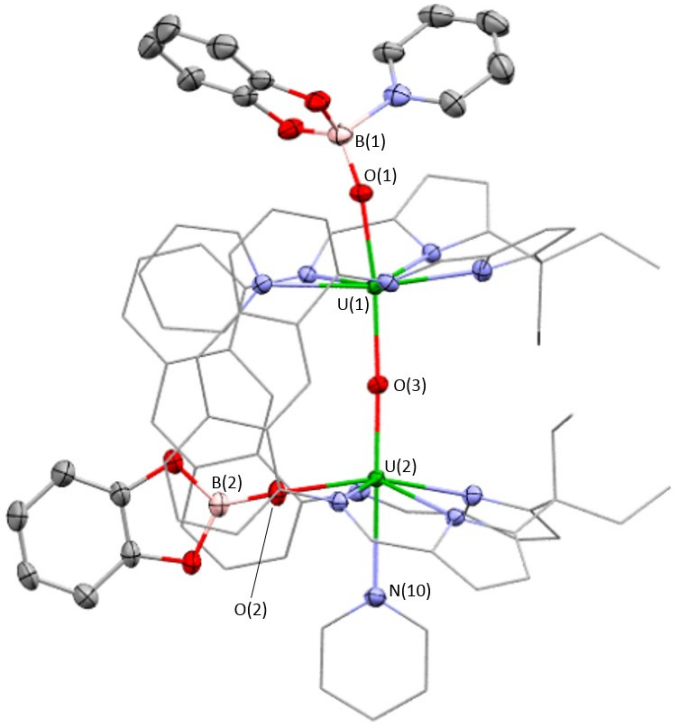

Figure S2. Solid-state structure of **3·THF** with thermal ellipsoids drawn at 50% probability, carbon atoms of the L^A ligand and U-coordinated solvent drawn wireframe, and hydrogen atoms and lattice solvent omitted for clarity. Key bond lengths [Å] and angles [°]: U(1)–O(1), 2.092(2); U(2)–O(2), 2.219(2); U(1)–O(3), 2.176(2); U(2)–O(3), 2.068(2); O(1)–B(1), 1.400(5); O(2)–B(2), 1.315(5); U(1)–N_{avg}, 2.545(7); U(2)–N_{avg}, 2.557(7); O(1)–U(1)–O(3), 170.7(1); O(2)–U(2)–O(3), 99.2(1); U(1)–O(3)–U(2), 177.6(1); B(1)–O(1)–U(1), 158.8(3); B(2)–O(2)–U(2), 171.1(3).

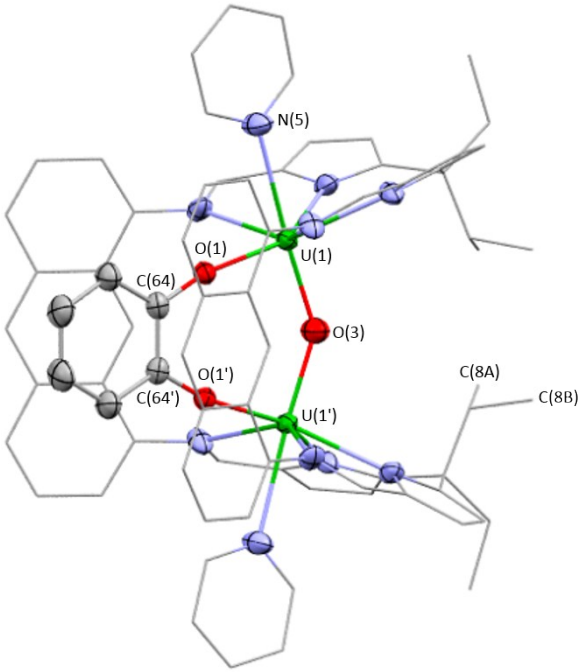

Figure S3. Solid-state structure of **4·5.5THF** with thermal ellipsoids drawn at 50% probability, carbon atoms of the L^A ligand and U-coordinated solvent drawn wireframe, and hydrogen atoms and lattice solvent omitted for clarity. C(8) is positionally disordered over two positions, so it's thermal parameters are split into two parts (labelled as C(8A) and C(8B) above) with an occupancy set to 0.5 for each. Key bond lengths [Å] and angles [°]: U(1)–O(1), 2.128(3); U(1)–O(3), 2.090(2); U(1)–N_{avg}, 2.56(1); C(64)–O(1), 1.340(6); O(1)–U(1)–O(3), 91.9(2); N(5)–U(1)–O(3), 176.8(2); U(1)–O(3)–U(1'), 142.3(3).

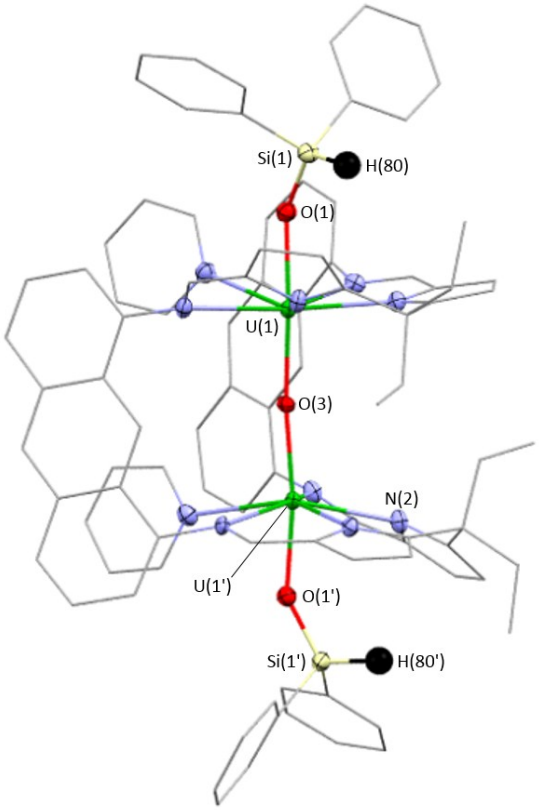

Figure S4. Solid-state structure of **5·py** with thermal ellipsoids drawn at 50% probability, carbon atoms of the L^A ligand, U-coordinated solvent and Si*H*Ph_2-phenyl groups drawn wireframe, and hydrogen atoms (except for H(80) and H(80')) and lattice solvent omitted for clarity. Key bond lengths [Å] and angles [°]: U(1)–O(1), 2.142(2); U(1)–O(3), 2.1486(3); U(1)–N_{avg}, 2.546(7); Si(1)–O(1), 1.623(3); O(1)–U(1)–O(3), 172.09(9); U(1)–O(3)–U(1'), 173.1(2); Si(1)–O(1)–U(1), 146.9(2).

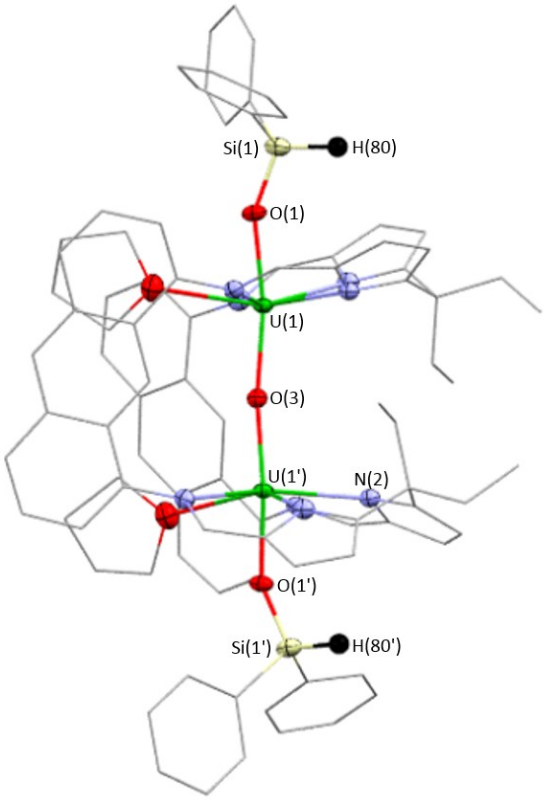

Figure S5. Solid-state structure of **5·2THF** with thermal ellipsoids drawn at 50% probability, carbon atoms of the L^A ligand, U-coordinated solvent and SiH*Ph*$_2$-phenyl groups drawn wireframe, and hydrogen atoms (except for H(80) and H(80')) and lattice solvent omitted for clarity. Key bond lengths [Å] and angles [°]: U(1)–O(1), 2.135(2); U(1)–O(3), 2.1425(3); U(1)–N_{avg}, 2.533(6); Si(1)–O(1), 1.620(2); O(1)–U(1)–O(3), 169.23(9); U(1)–O(3)–U(1'), 172.0(2); Si(1)–O(1)–U(1), 154.0(2).

NMR Spectra

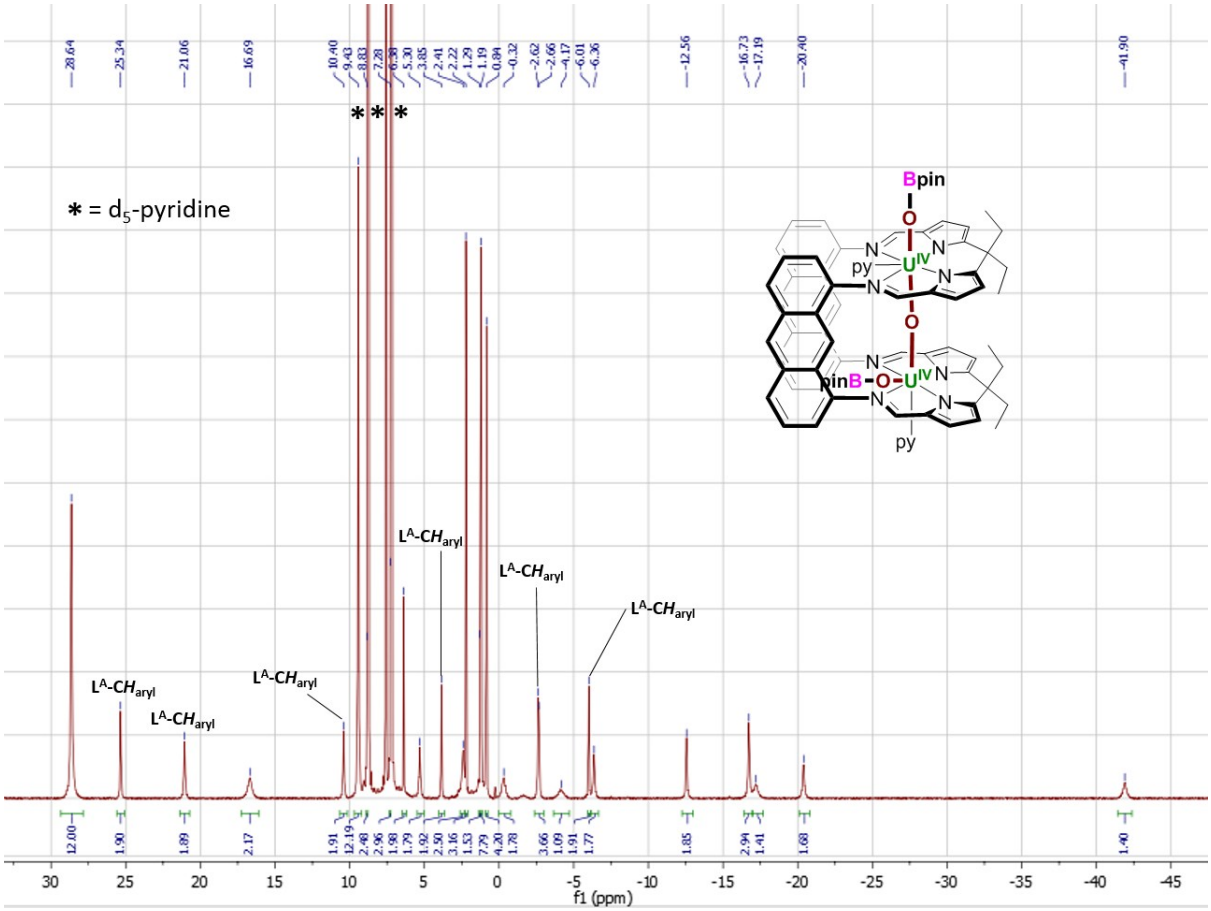

Figure S6. ^{1}H NMR spectrum of **2** (500 MHz; d_5-pyridine; 298 K; $SiMe_4$).

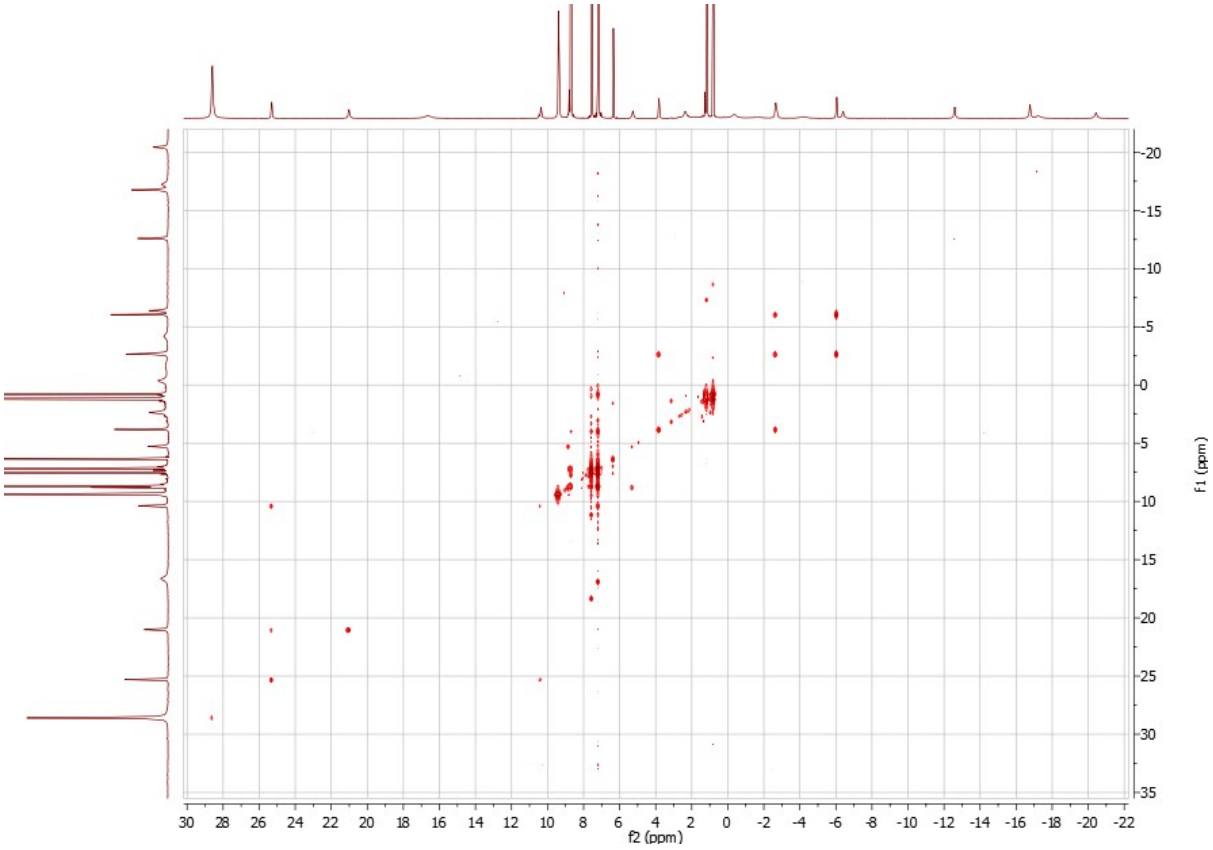

Figure S7. $^{1}H,^{1}H$-COSY NMR spectrum of **2** (600 MHz; d_5-pyridine; 298 K; $SiMe_4$).

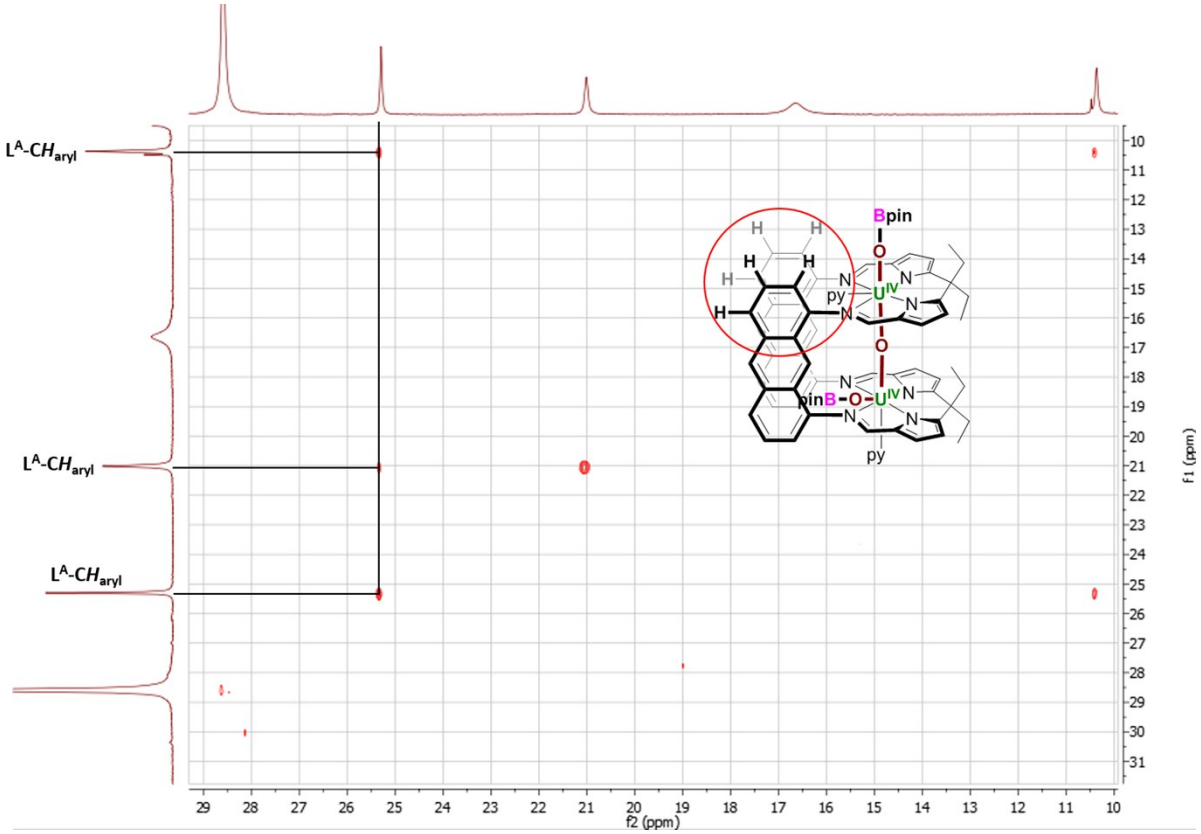

Figure S8. Expanded view of the ^{1}H,^{1}H-COSY NMR spectrum of **2** (600 MHz; d_5-pyridine; 298 K; $SiMe_4$), displaying 1 of 2 sets of L^A-CH_{aryl} coupling observed within the anthracenyl ligand backbone. Each signal integrates to two protons (as opposed to four), indicating there is side-to-side symmetry but not both side-to-side and top-bottom symmetry, consistent with one OBpin ligand coordinated to U in an axial position and the other coordinated in an equatorial position.

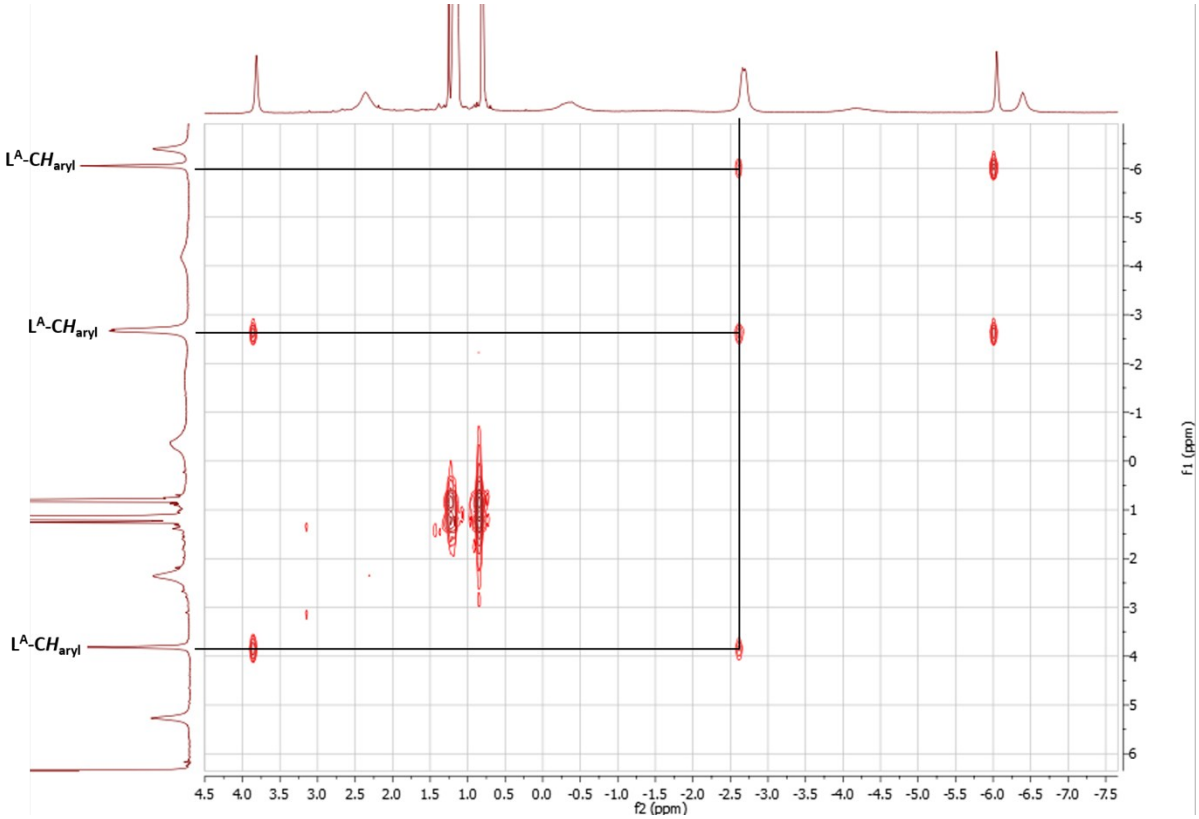

Figure S9. Expanded view of the ^{1}H,^{1}H-COSY NMR spectrum of **2** (600 MHz; d_5-pyridine; 298 K; $SiMe_4$), displaying the second of 2 sets of L^A-CH_{aryl} coupling observed within the anthracenyl ligand backbone.

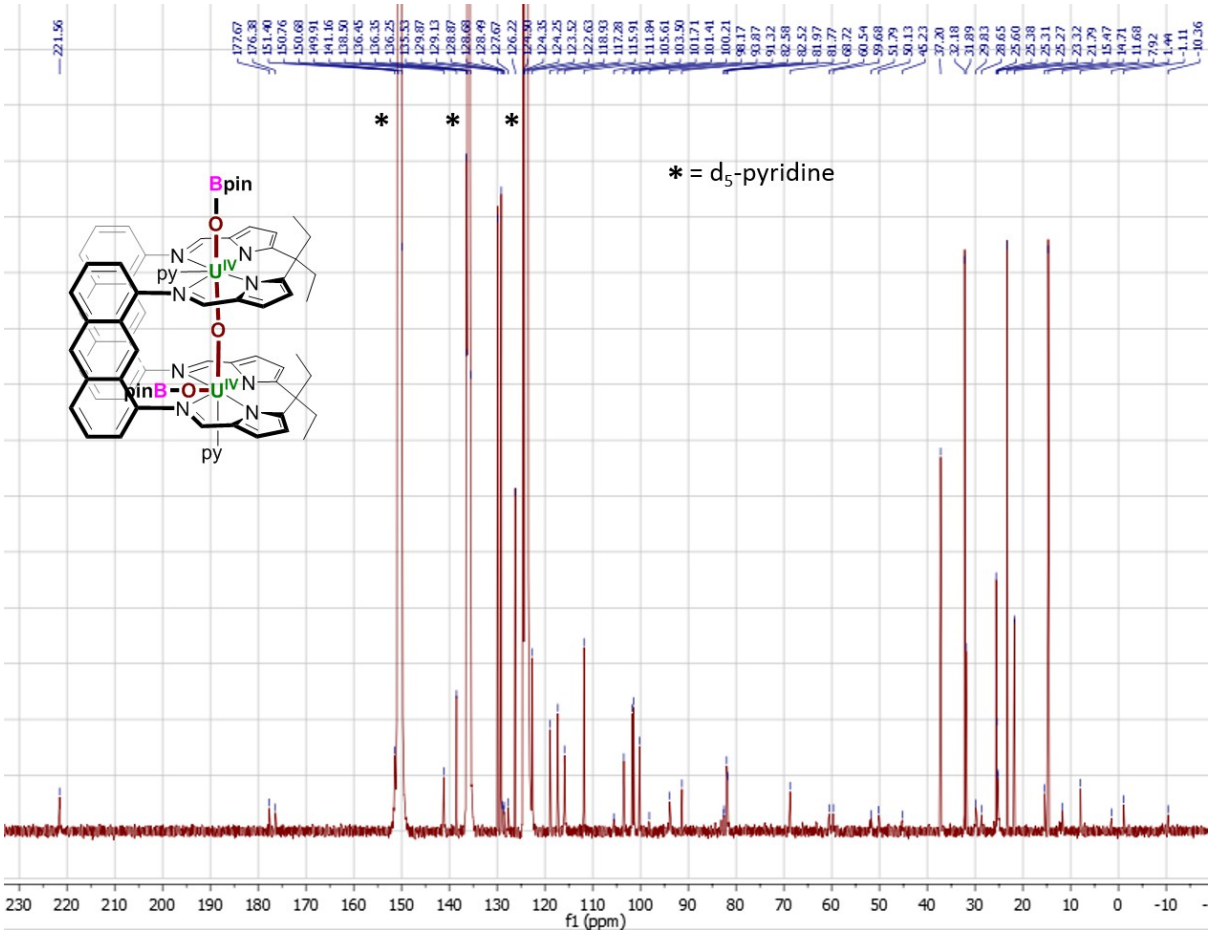

Figure S10. $^{13}C\{^{1}H\}$ NMR spectrum of **2** (126 MHz; d_5-pyridine; 298 K; $SiMe_4$).

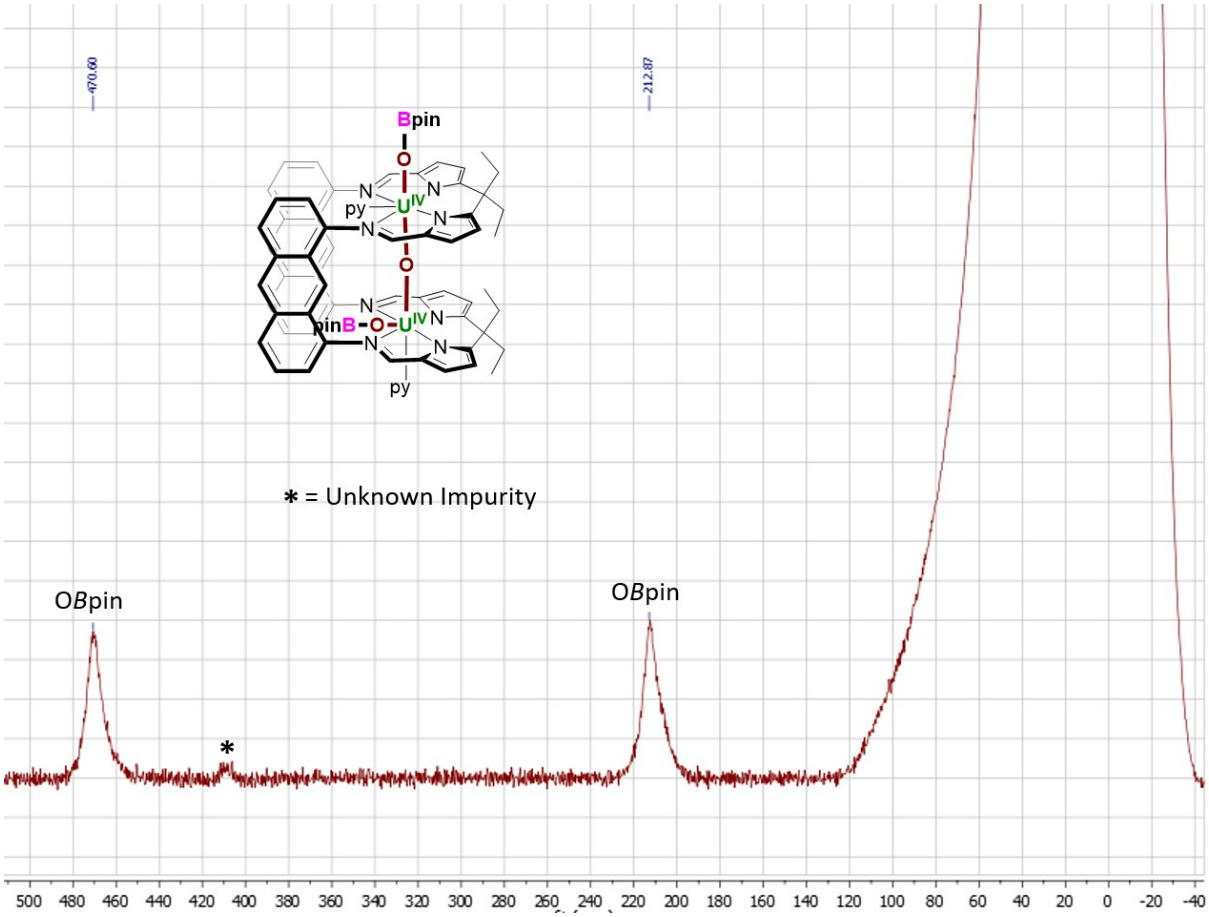

Figure S11. ^{11}B NMR spectrum of **2** (161 MHz; C_6D_6; 298 K; $BF_3(OEt_2)$).

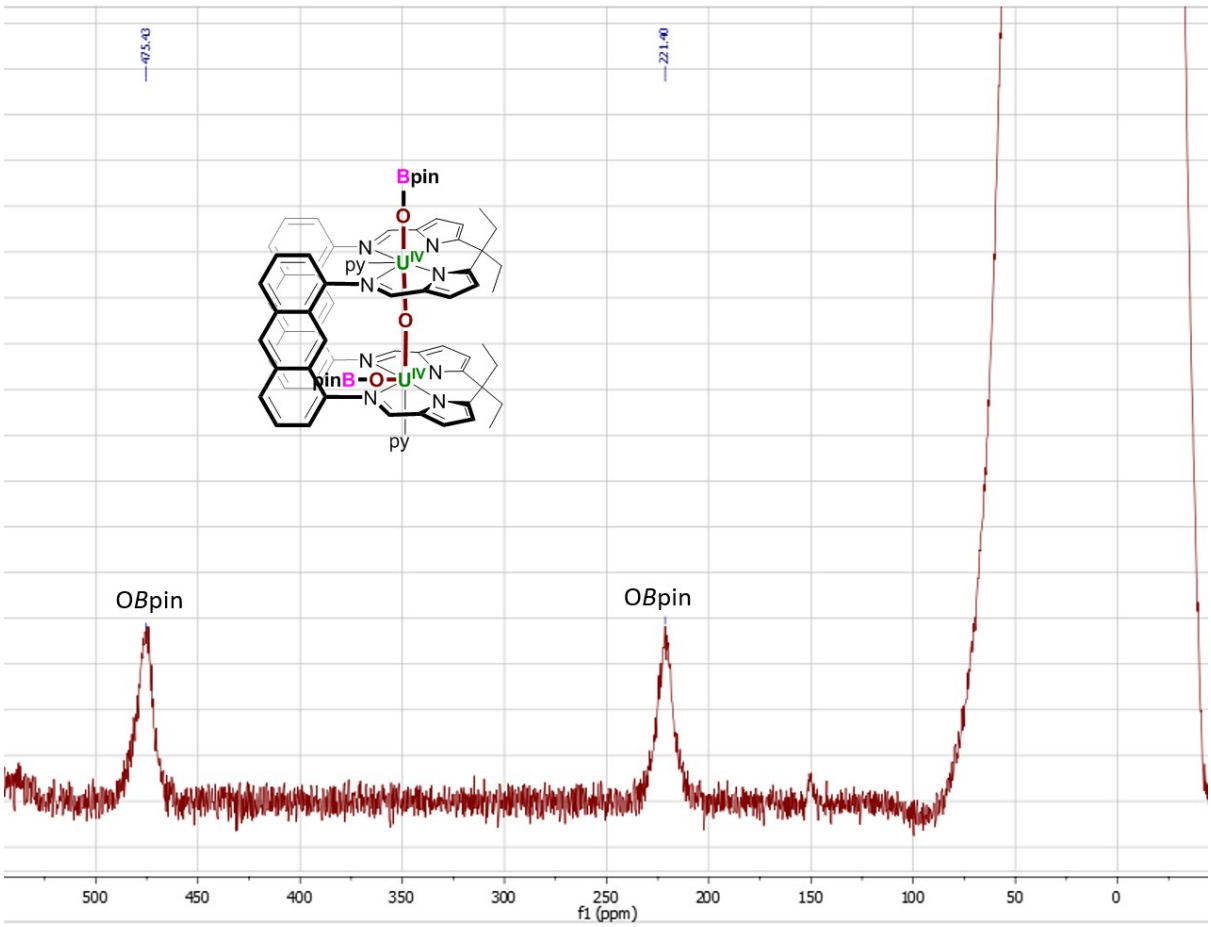

Figure S12. ^{11}B NMR spectrum of **2** (161 MHz; d_5-pyridine; 298 K; $BF_3(OEt_2)$).

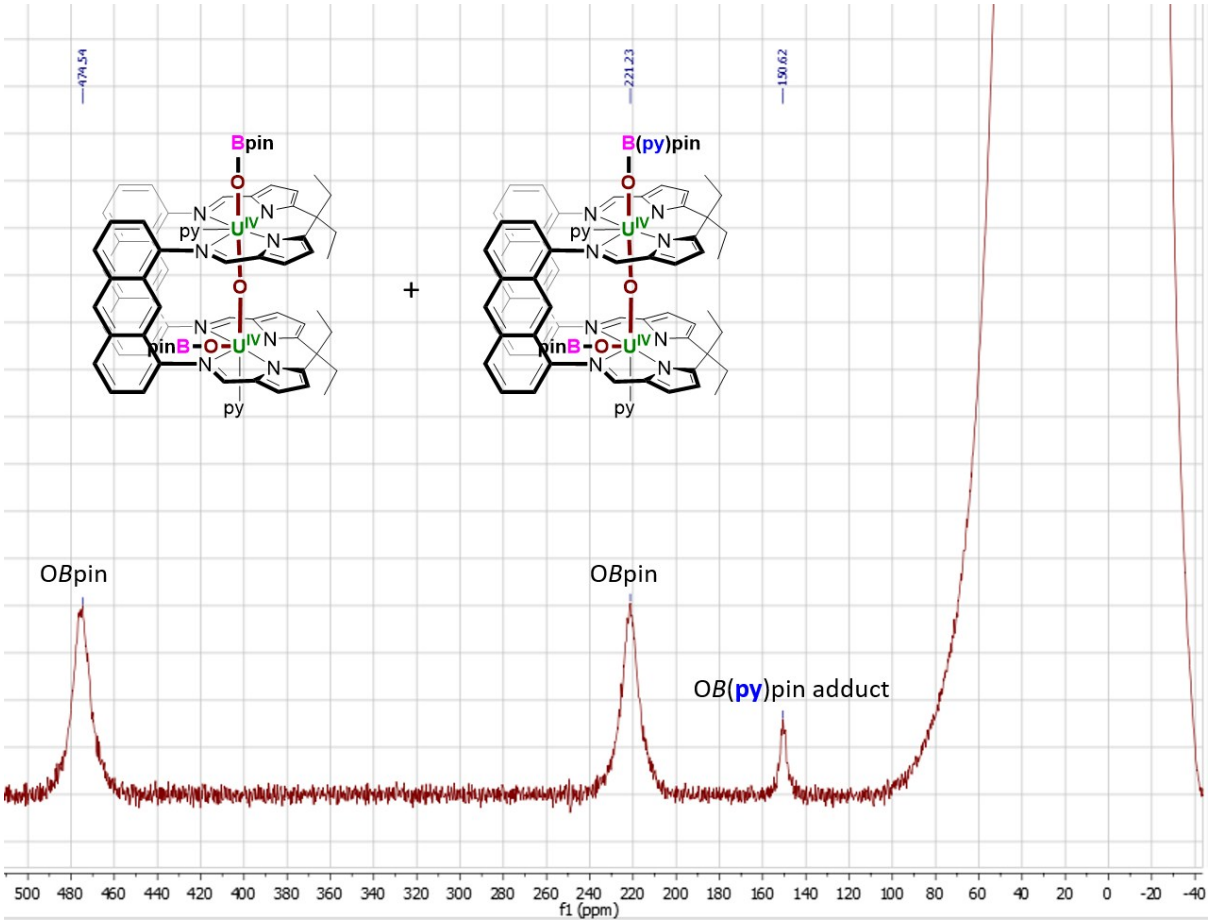

Figure S13. ^{11}B NMR spectrum of **2** stored in d_5-pyridine for one day (161 MHz; d_5-pyridine; 298 K; $BF_3(OEt_2)$). An ^{11}B signal at 151 ppm has emerged, and is identified as the pyridine→Bpin adduct.

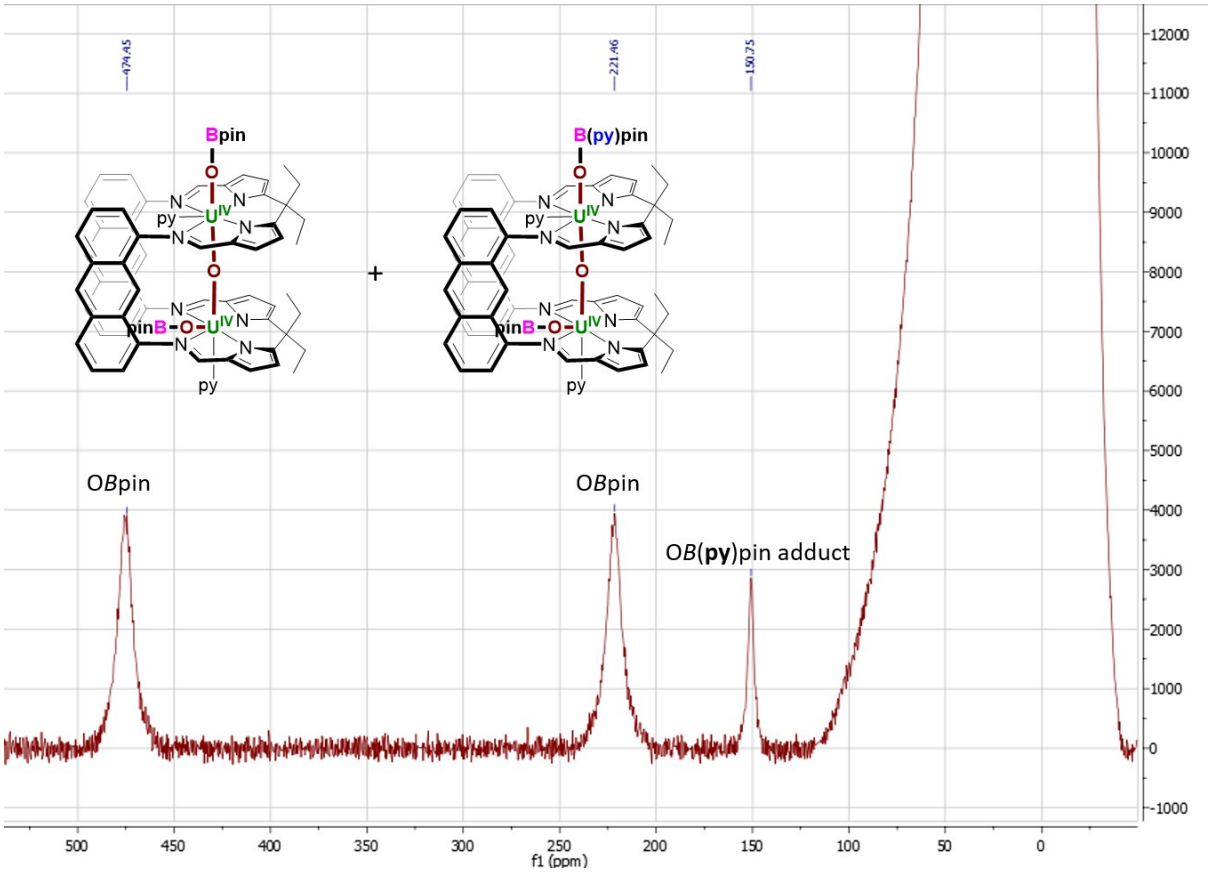

Figure S14. ^{11}B NMR spectrum of **2** stored in d_5-pyridine for one week (161 MHz; d_5-pyridine; 298 K; $BF_3(OEt_2)$). The ^{11}B signal at 151 ppm has grown in intensity over time.

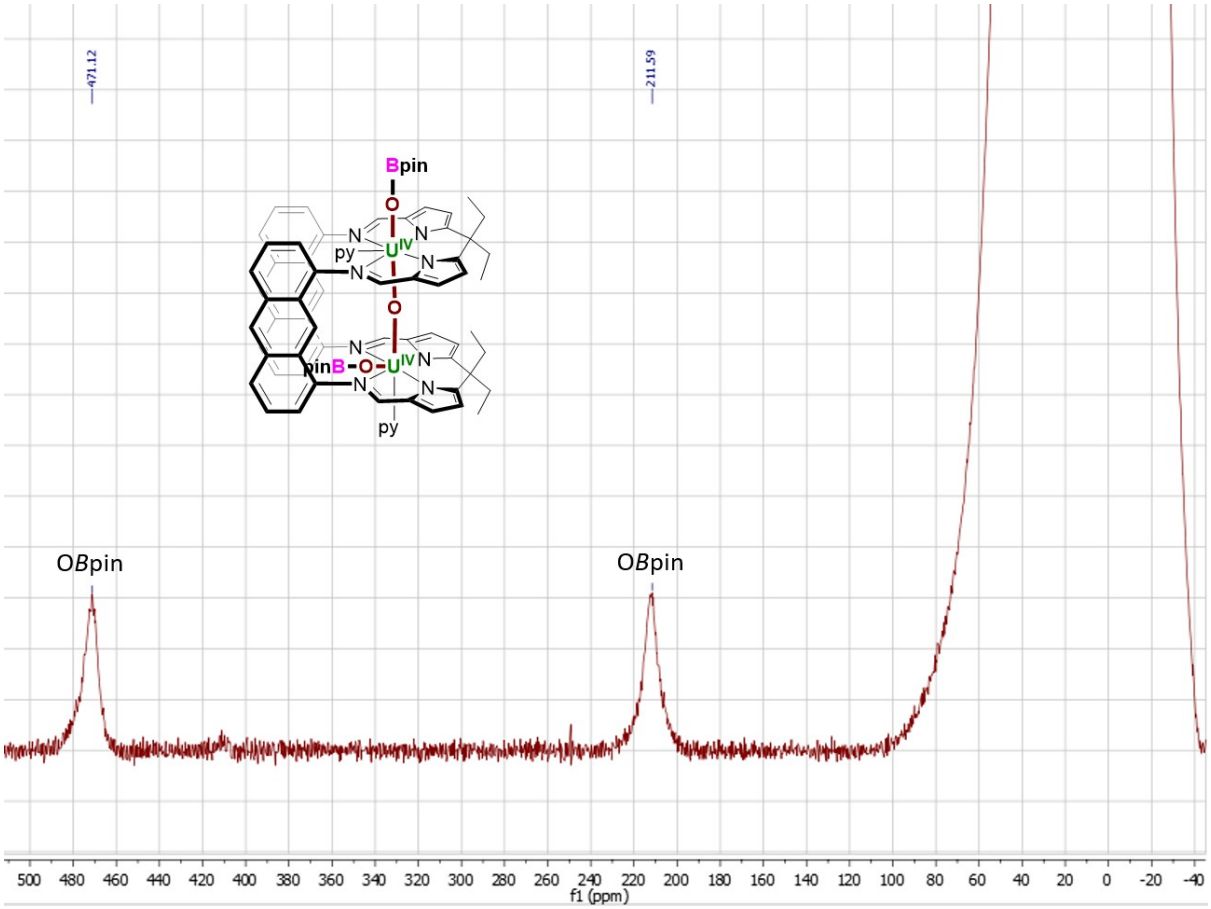

Figure S15. ^{11}B NMR spectrum of **2** in C_6D_6 after being evaporated to dryness under reduced pressure from a d_5-pyridine solution (161 MHz; C_6D_6; 298 K; $BF_3(OEt_2)$). The ^{11}B NMR signal at 151 ppm in d_5-pyridine is no longer present, indicating pyridine→Bpin adduct formation is labile.

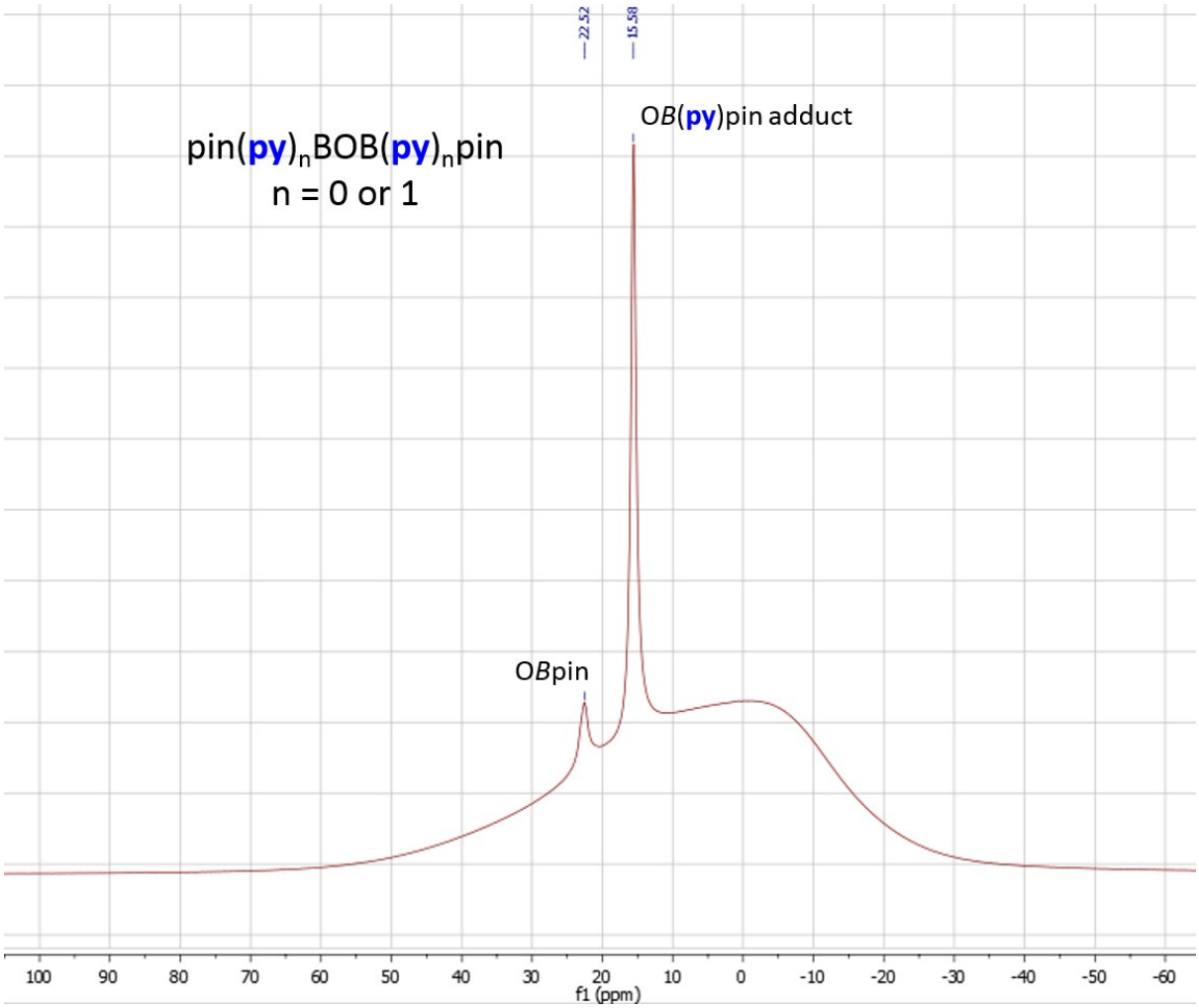

Figure S16. ^{11}B NMR spectrum of pin(py)$_n$BOB(py)$_n$pin (n = 0, 1), generated by adding Me_3NO to B_2pin_2 and used to identify the byproducts produced during the formation of **2** (161 MHz; d_5-pyridine; 298 K; $BF_3(OEt_2)$).

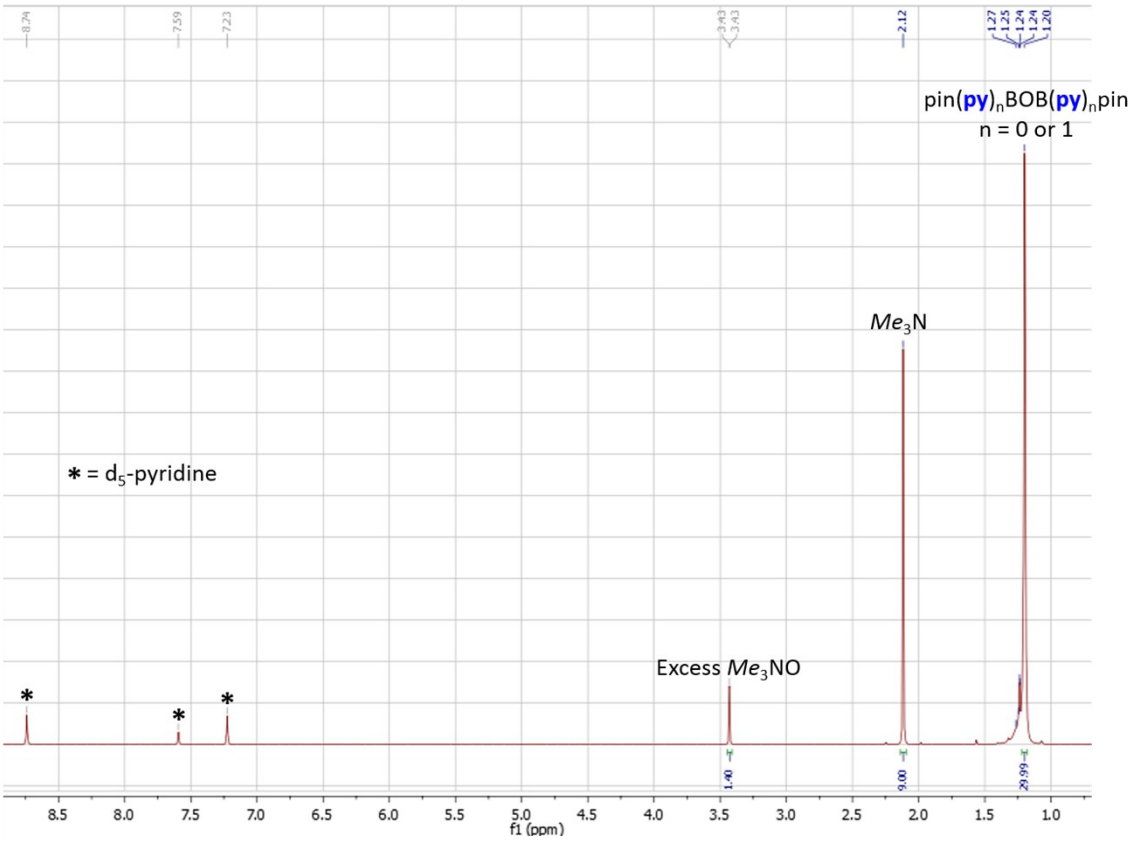

Figure S17. ^{1}H NMR spectrum of pin(py)$_n$BOB(py)$_n$pin (n = 0, 1), generated by adding Me_3NO to B_2pin_2 and used to identify the byproducts produced during the formation of **2** (500 MHz; d_5-pyridine; 298 K; $SiMe_4$).

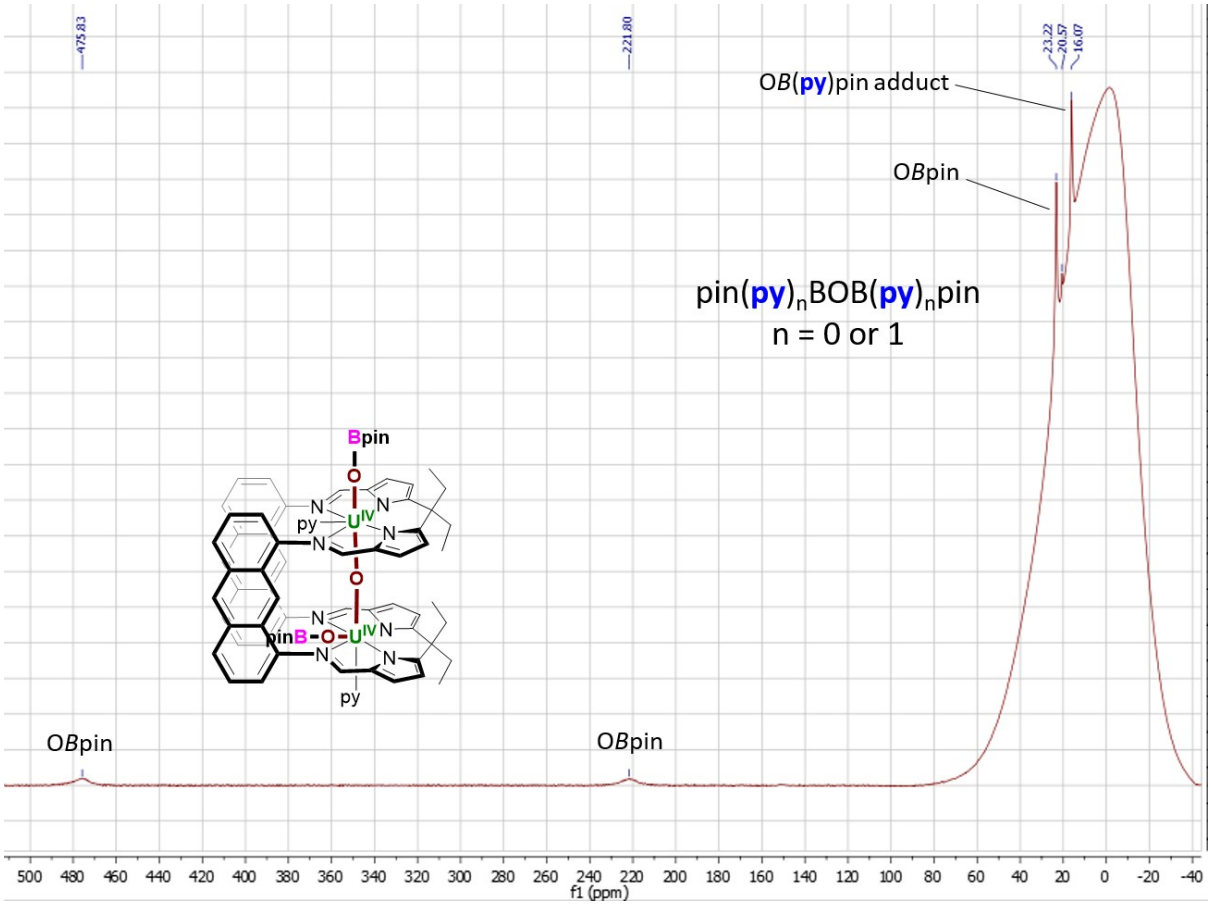

Figure S18. ^{11}B NMR spectrum of **2** generated *in-situ*; pin(py)$_n$BOB(py)$_n$pin (n = 0, 1) are the byproducts observed during the formation of **2** (161 MHz; d_5-pyridine; 298 K; $BF_3(OEt_2)$).

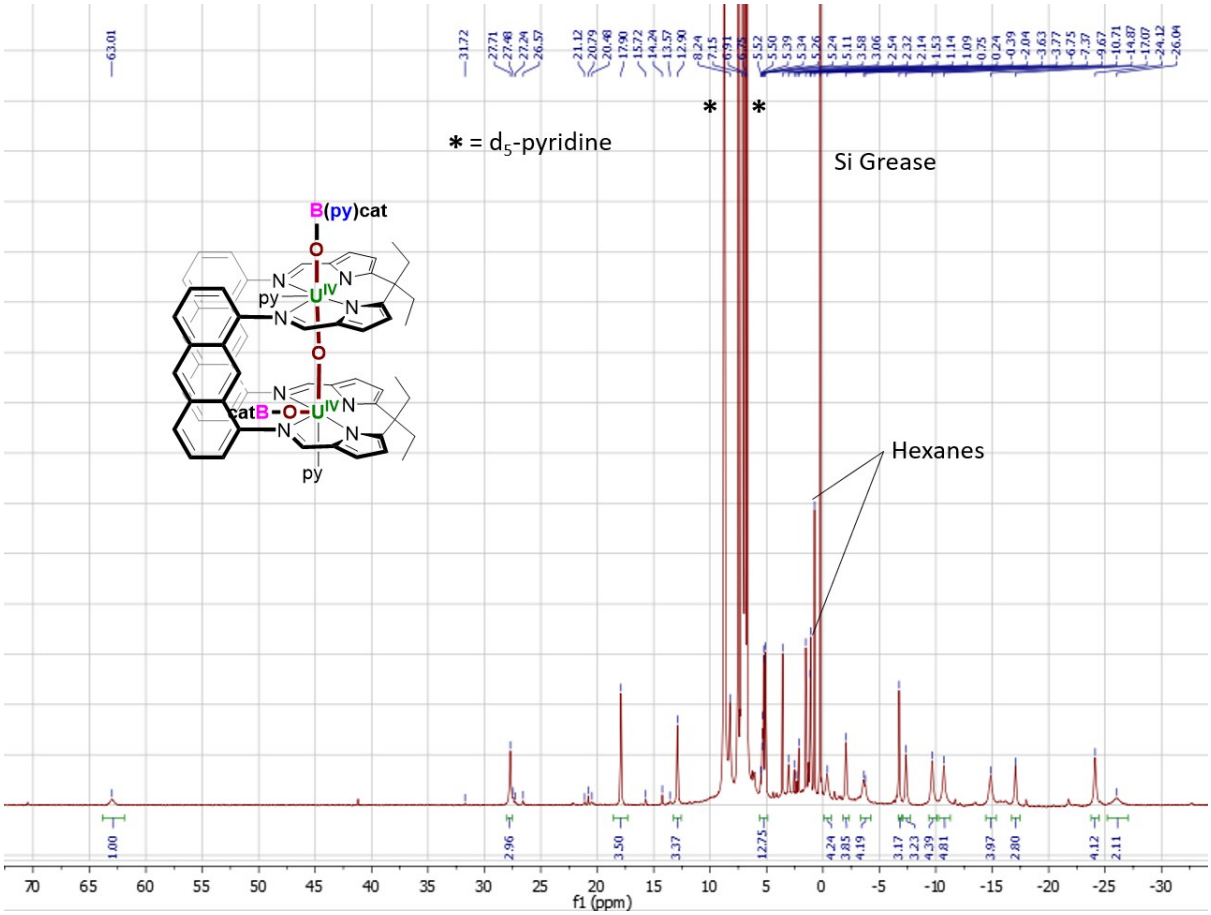

Figure S19. ^{1}H NMR spectrum of **3** generated *in-situ* (500 MHz; d_5-pyridine; 298 K; $SiMe_4$).

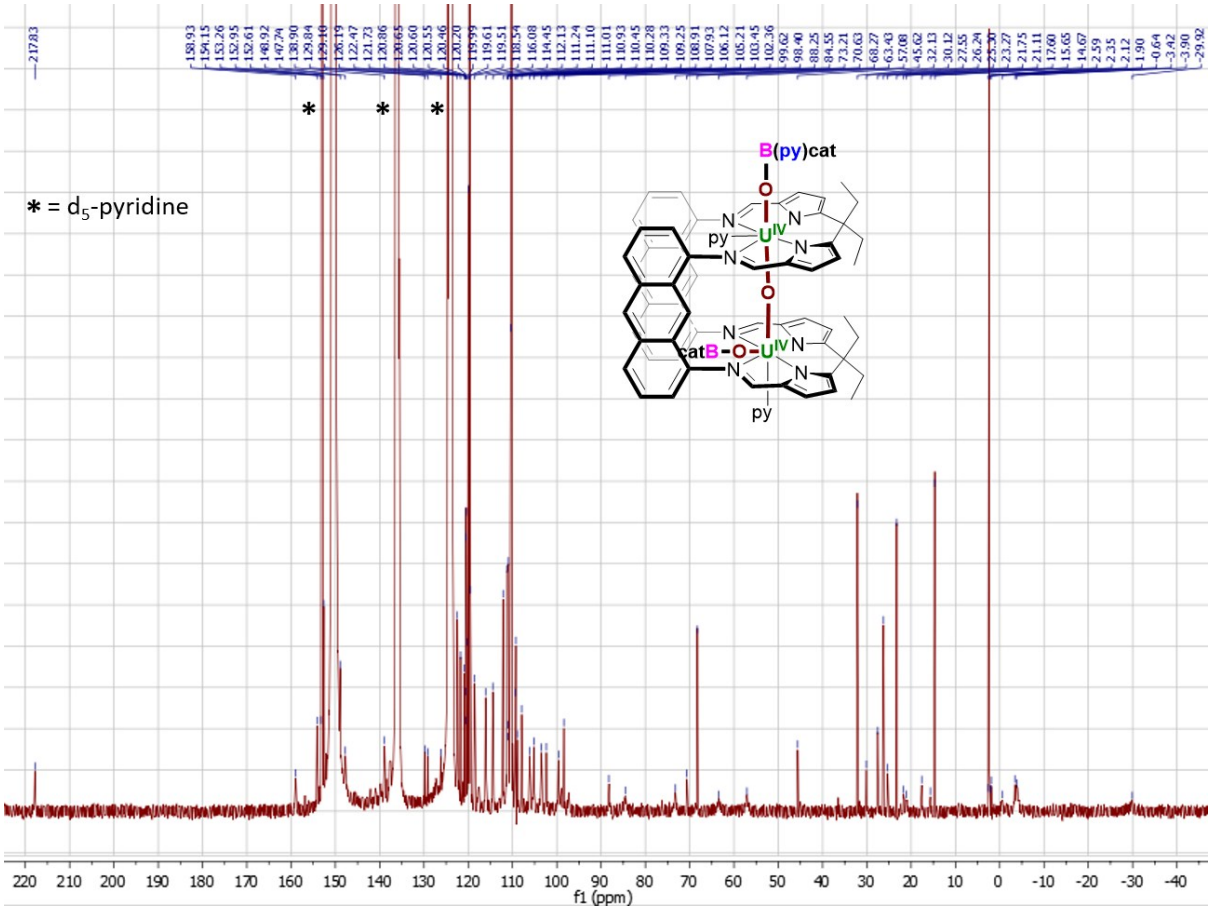

Figure S20. $^{13}C\{^{1}H\}$ NMR spectrum of **3** generated *in-situ* (126 MHz; d_5-pyridine; 298 K; $SiMe_4$).

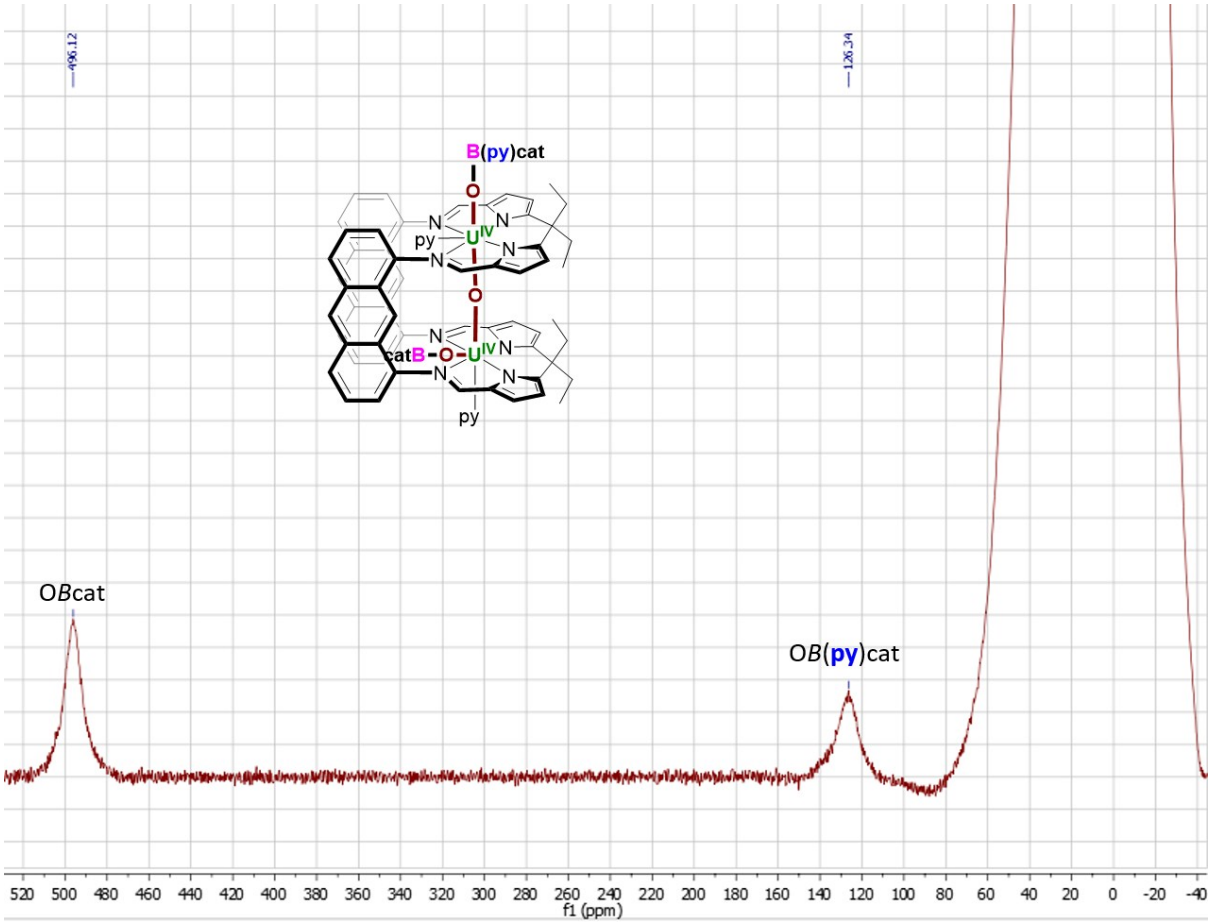

Figure S21. ^{11}B NMR spectrum of **3** generated *in-situ* (161 MHz; d_5-pyridine; 298 K; $BF_3(OEt_2)$).

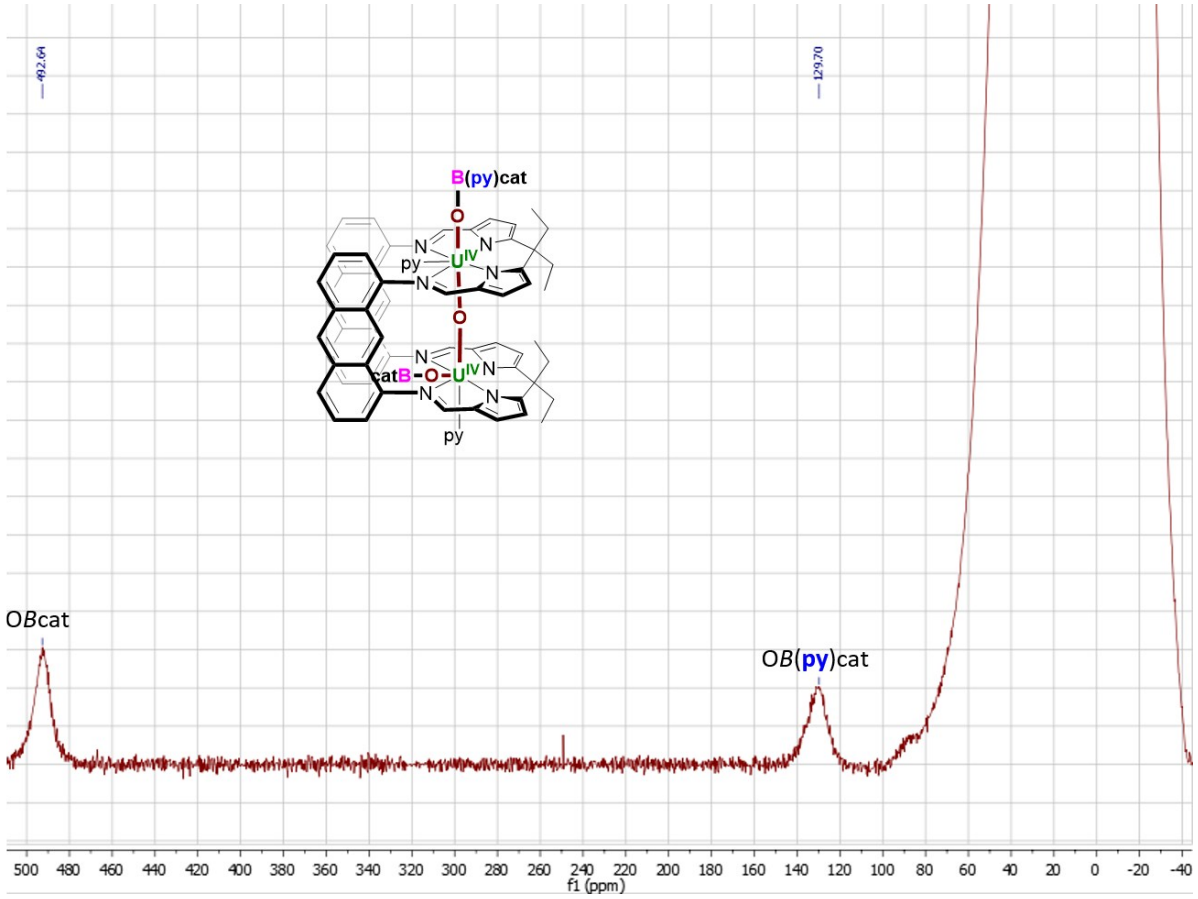

Figure S22. ^{11}B NMR spectrum of **3** generated *in-situ* (161 MHz; C_6D_6; 298 K; $BF_3(OEt_2)$).

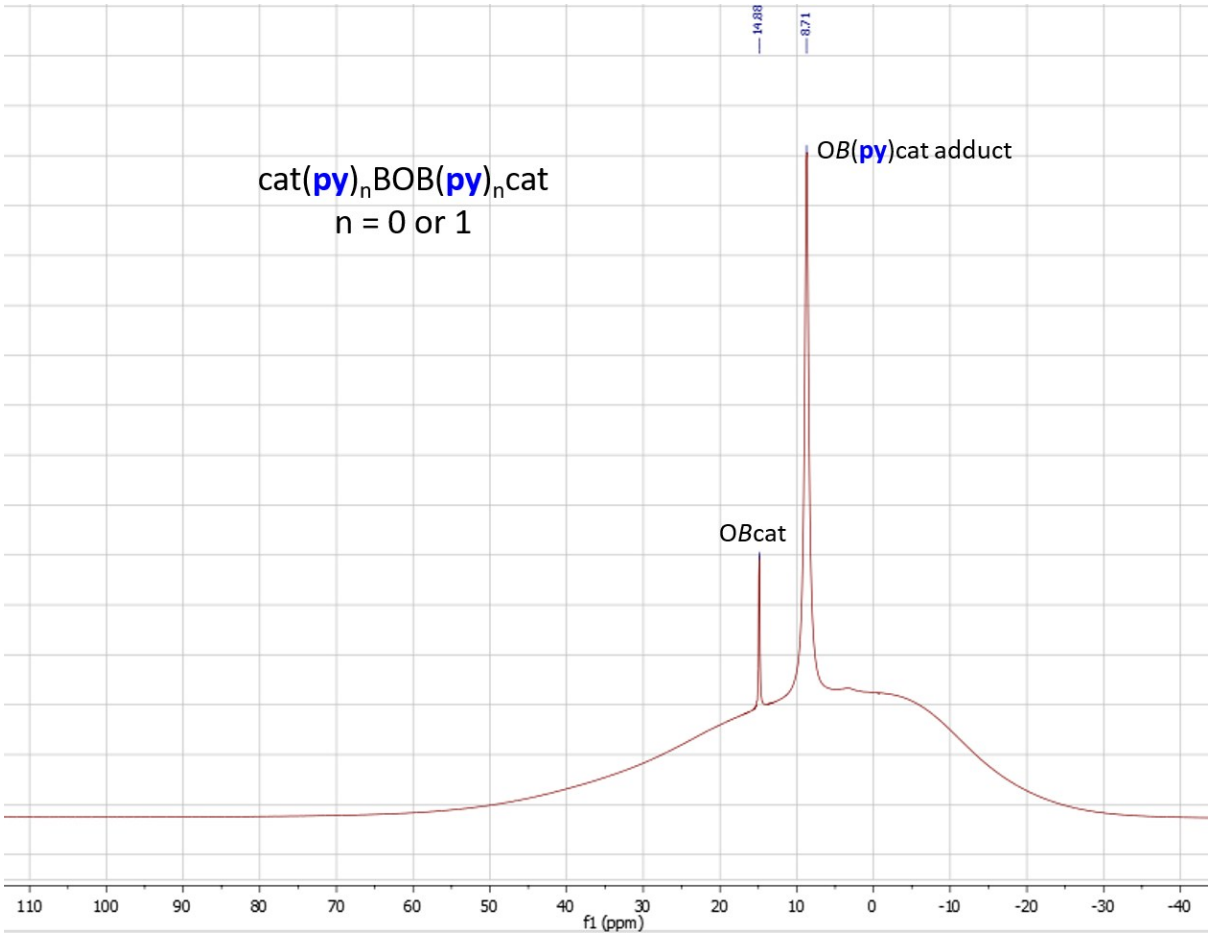

Figure S23. ^{11}B NMR spectrum of cat(py)$_n$BOB(py)$_n$cat (n = 0, 1), generated by adding Me_3NO to B_2cat_2 and used to identify the byproducts produced during the formation of **3** (161 MHz; d_5-pyridine; 298 K; $BF_3(OEt_2)$).

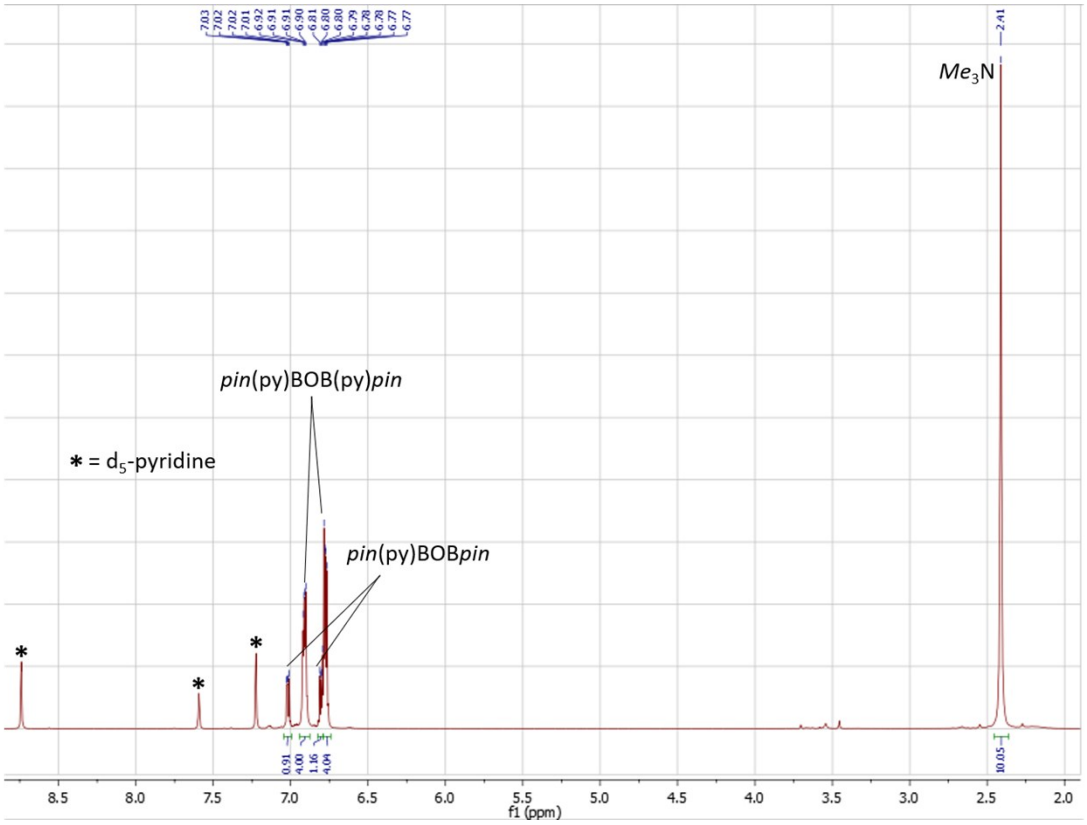

Figure S24. ^{1}H NMR spectrum of cat(py)$_n$BOB(py)$_n$cat (n = 0, 1), generated by adding Me_3NO to B_2cat_2 and used to identify the byproducts produced during the formation of **3** (500 MHz; d_5-pyridine; 298 K; $SiMe_4$).

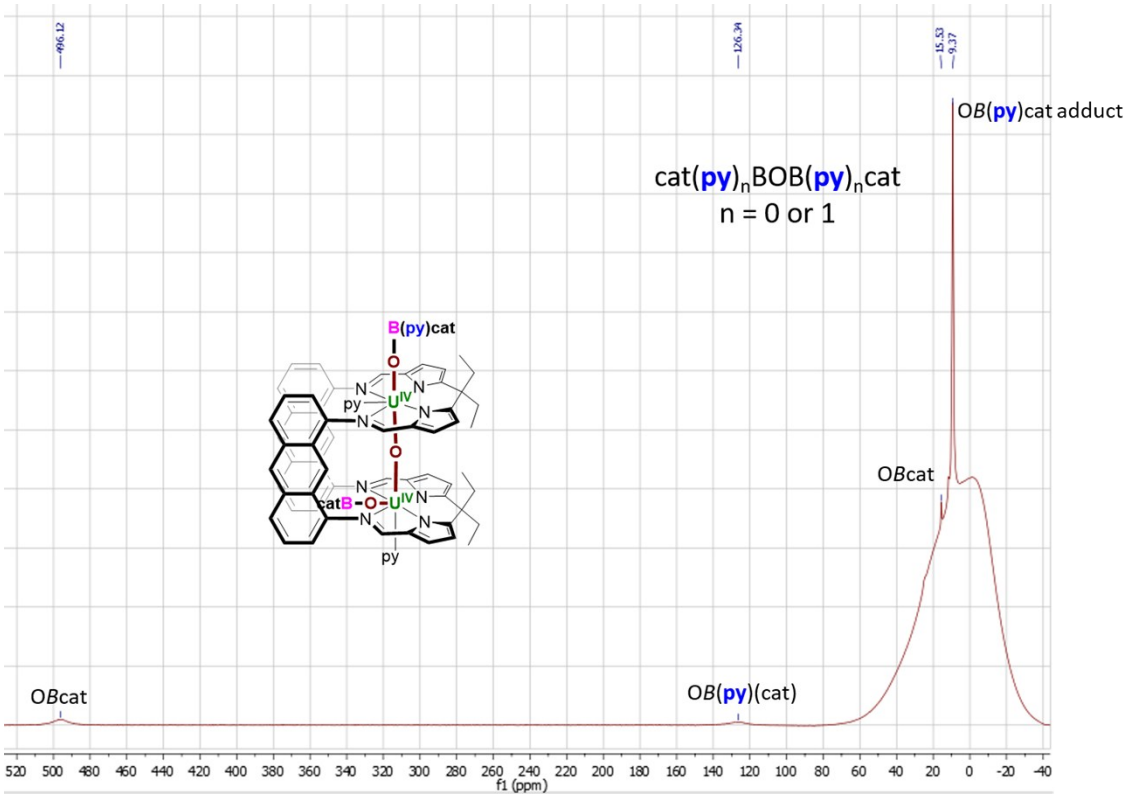

Figure S25. ^{11}B NMR spectrum of **3** generated *in-situ*; cat(py)$_n$BOB(py)$_n$cat (n = 0, 1) are the byproducts observed during the formation of **3** (161 MHz; d_5-pyridine; 298 K; $BF_3(OEt_2)$).

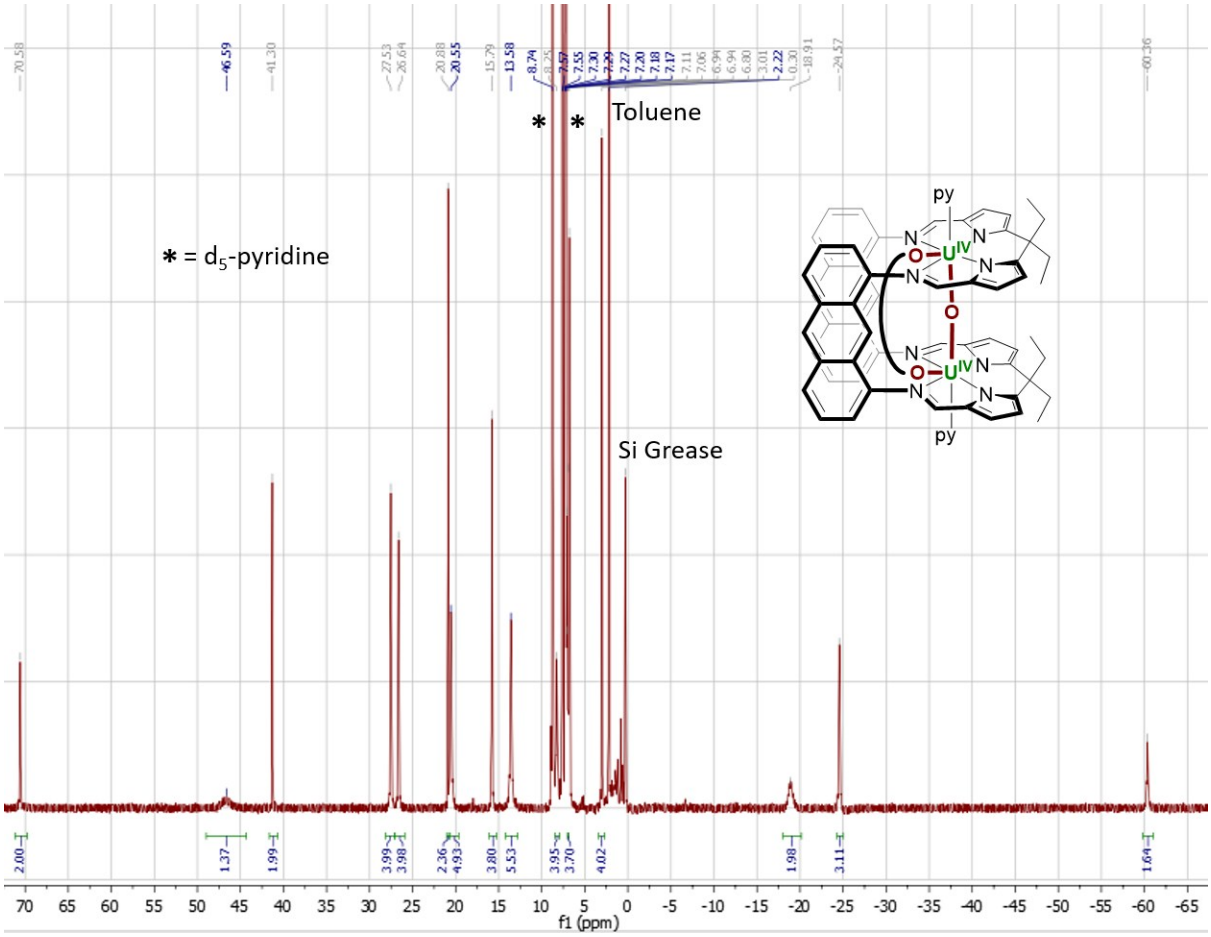

Figure S26. ^{1}H NMR spectrum of **4** (500 MHz; d_5-pyridine; 298 K; $SiMe_4$).

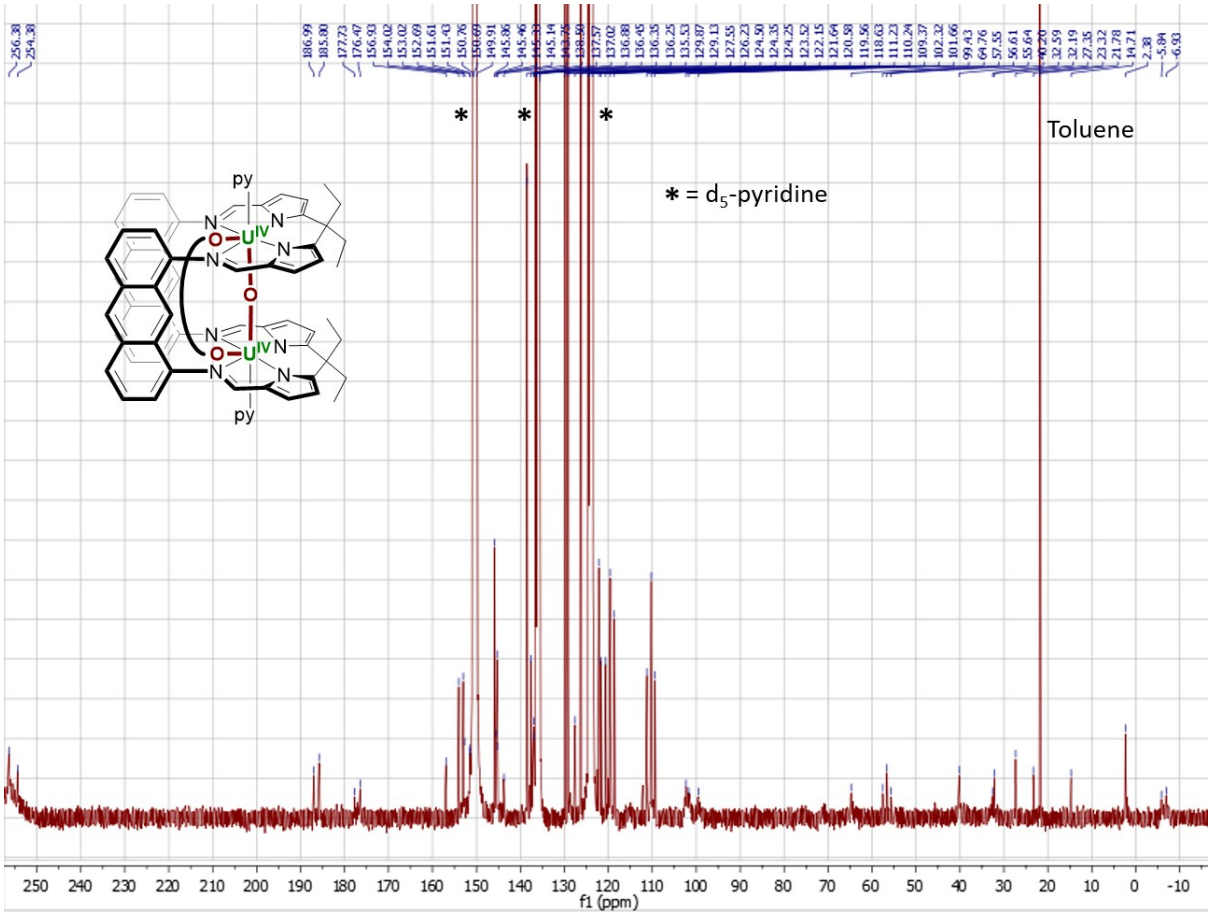

Figure S27. $^{13}C\{^{1}H\}$ NMR spectrum of **4** (126 MHz; d_5-pyridine; 298 K; $SiMe_4$).

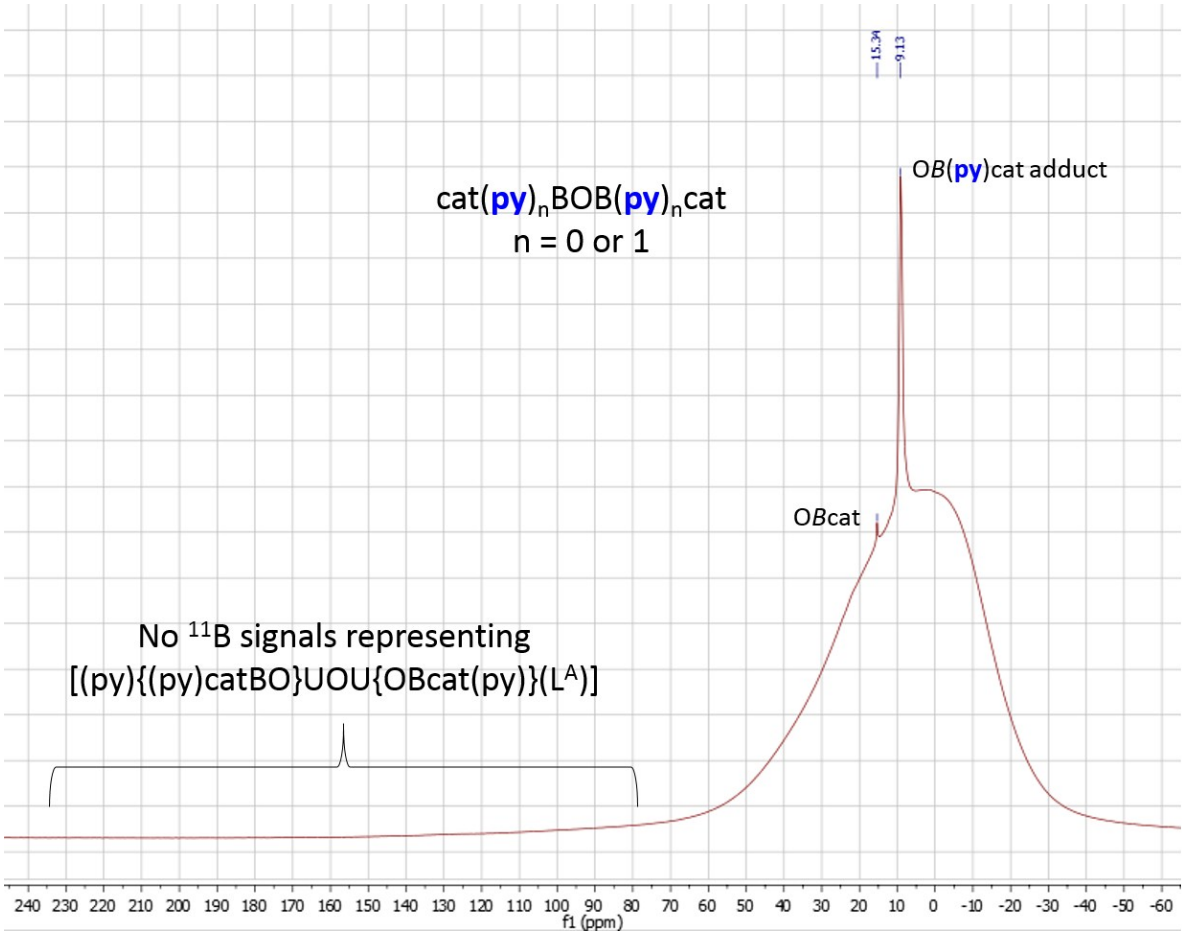

Figure S28. ^{11}B NMR spectrum of **4** generated *in-situ* (161 MHz; d_5-pyridine; 298 K; $BF_3(OEt_2)$). The absence of any ^{11}B signal between 500-100 ppm indicates that all of **3** is consumed during the formation of **4**.

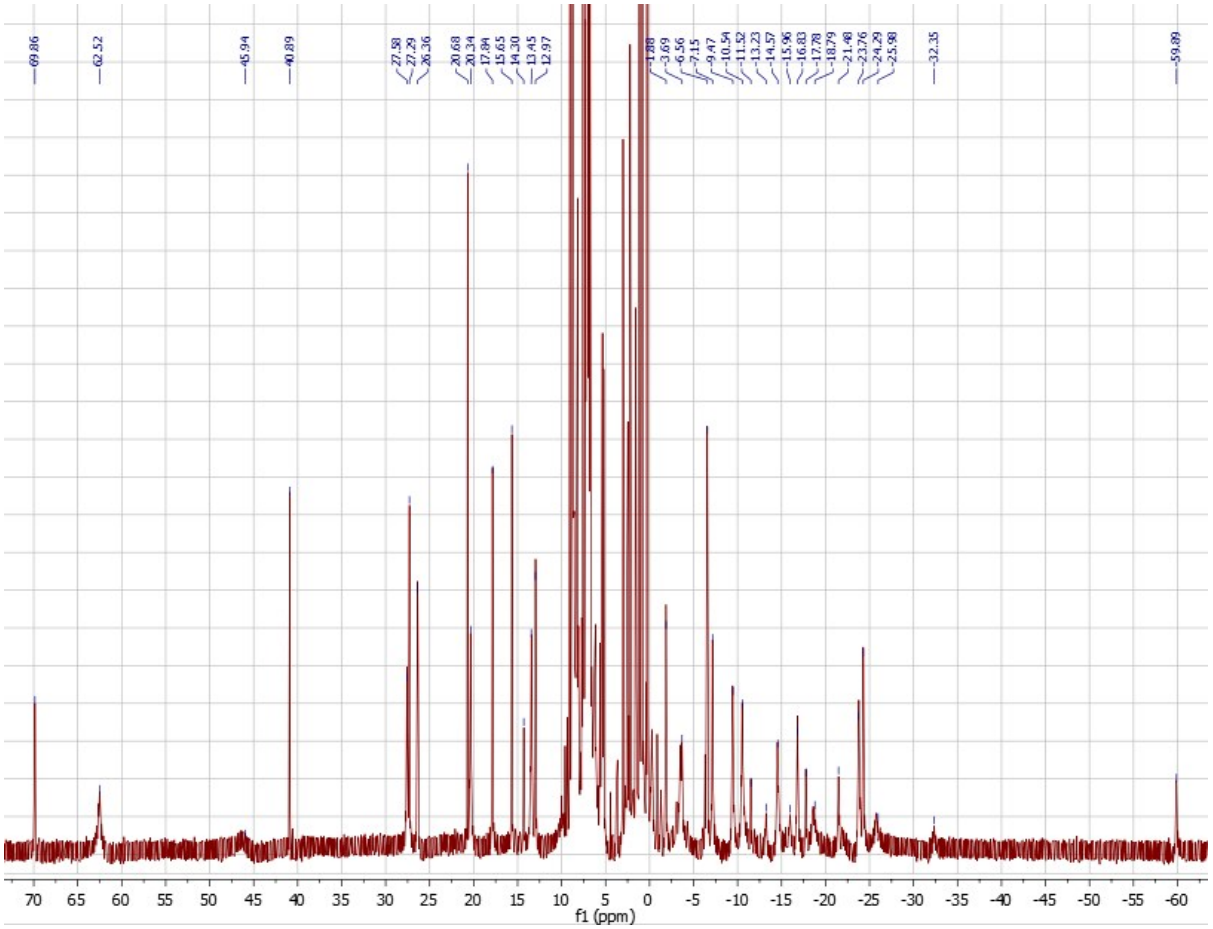

Figure S29. ^{1}H NMR spectrum of **1** + 3 equiv. B_2cat_2 heated to 80 ºC for 24 hours (500 MHz; d_5-pyridine; 298 K; $SiMe_4$). A mixture of **1**, **3** and **4** is observed.

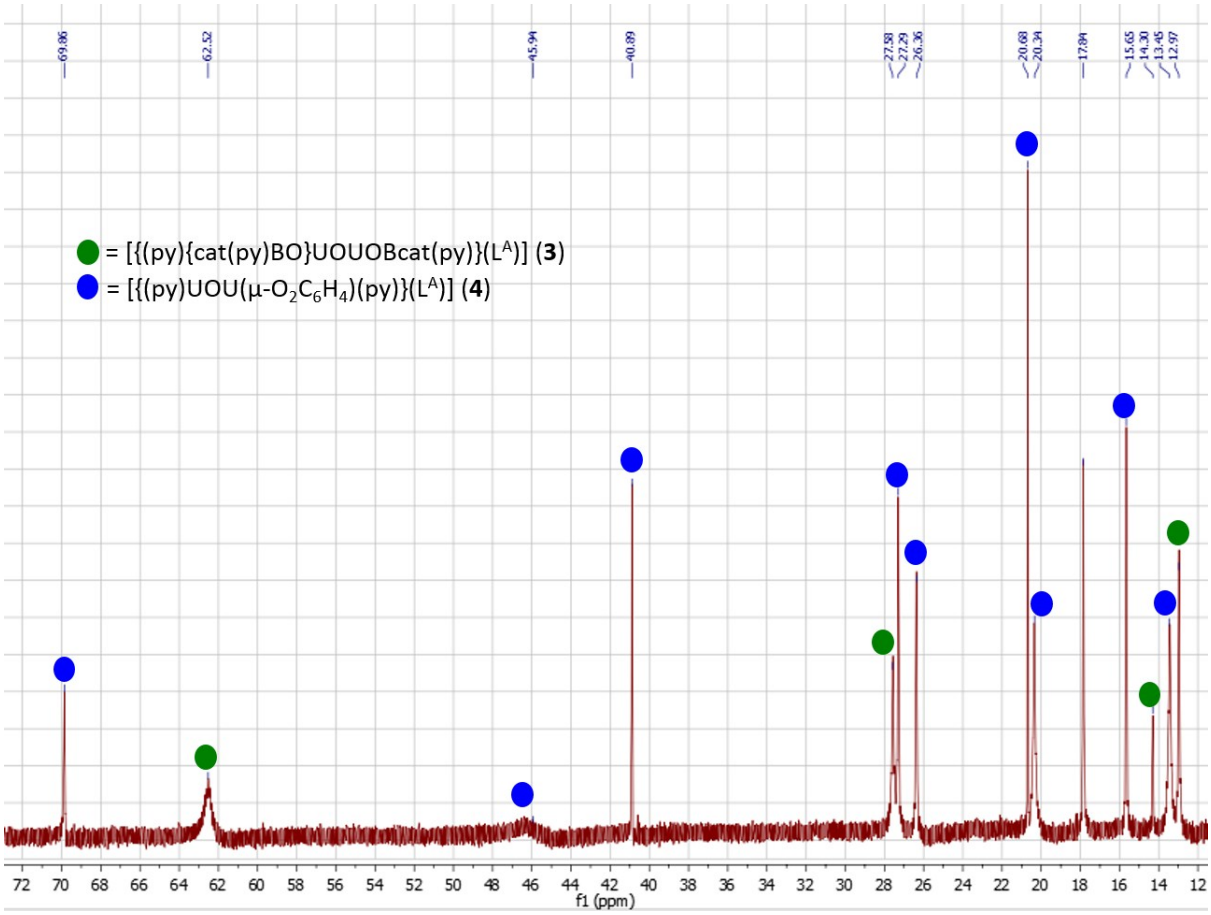

Figure S30. Expanded view of the ^{1}H NMR spectrum of **1** + 3 equiv. B_2cat_2 heated to 80 ºC for 24 hours (500 MHz; d_5-pyridine; 298 K; $SiMe_4$). A mixture of **1**, **3** and **4** is observed.

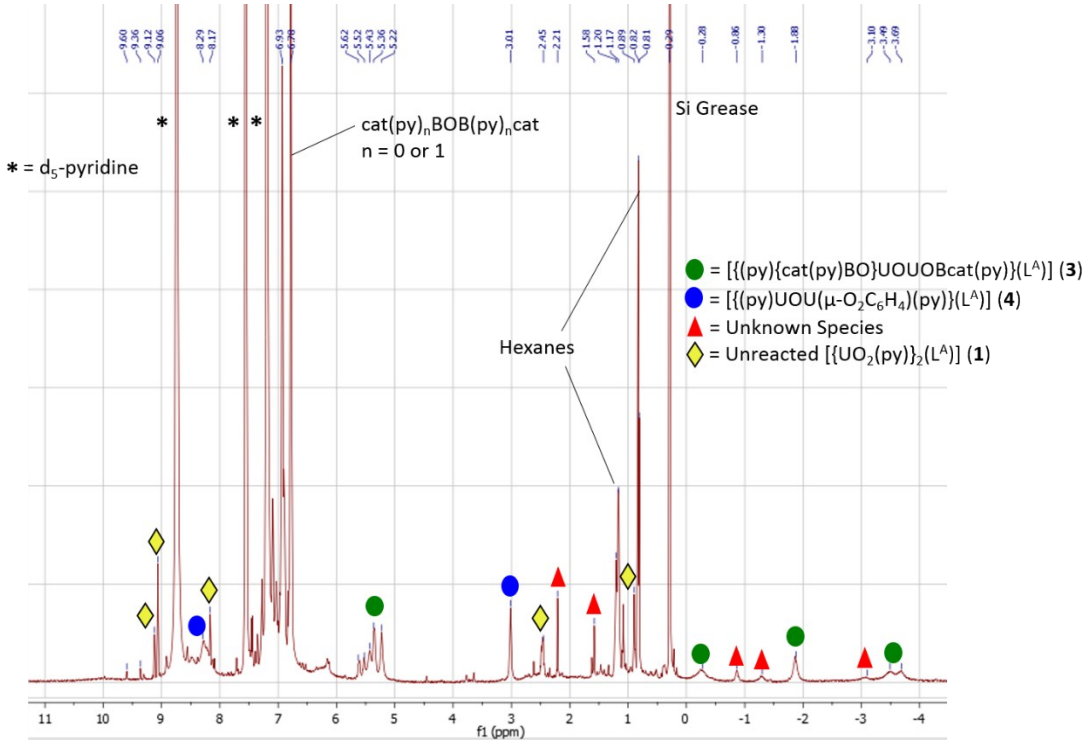

Figure S31. Expanded view of the ^{1}H NMR spectrum of **1** + 3 equiv. B_2cat_2 heated to 80 ºC for 24 hours (500 MHz; d_5-pyridine; 298 K; $SiMe_4$). A mixture of **1**, **3** and **4** is observed.

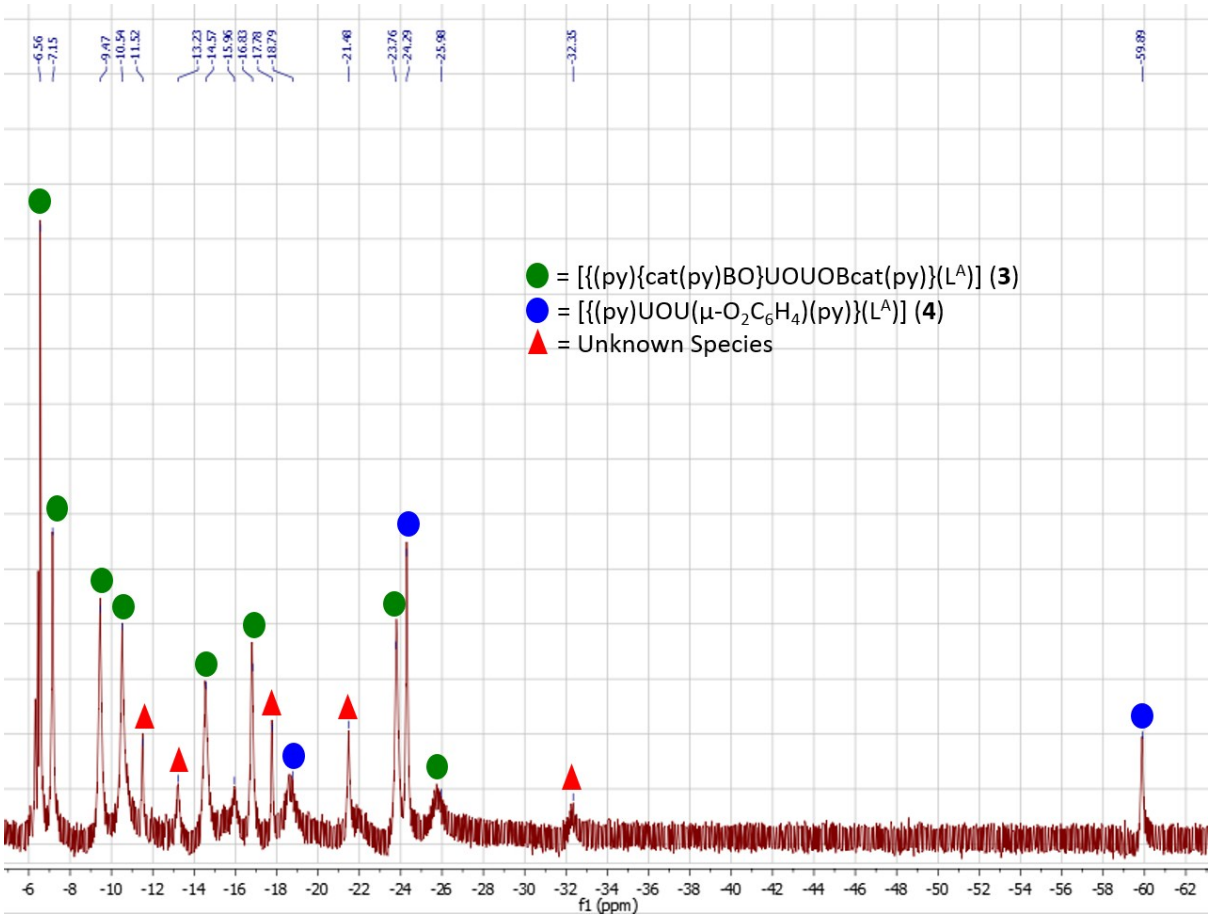

Figure S32. Expanded view of the ^{1}H NMR spectrum of **1** + 3 equiv. B_2cat_2 heated to 80 ºC for 24 hours (500 MHz; d_5-pyridine; 298 K; $SiMe_4$). A mixture of **1**, **3** and **4** is observed.

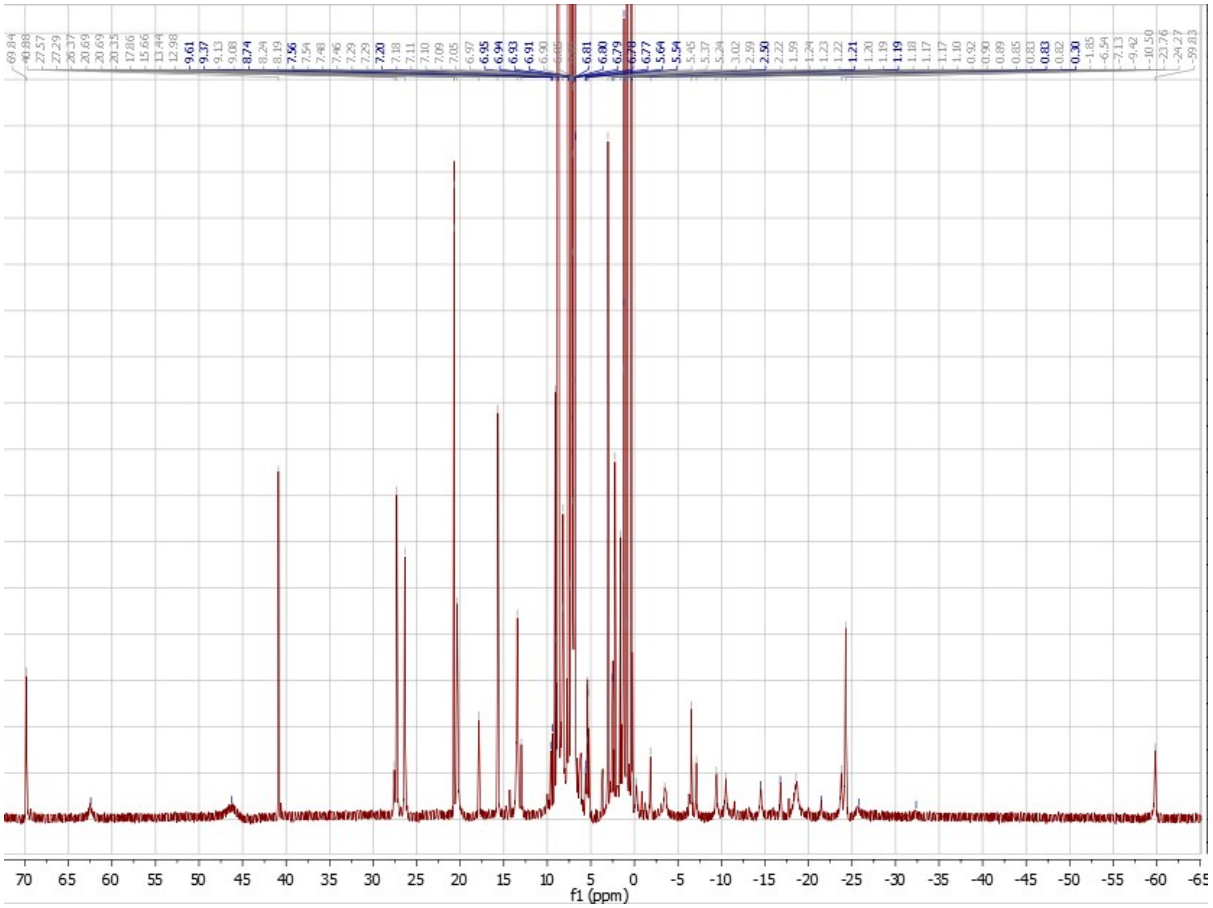

Figure S33. ^{1}H NMR spectrum of **1** + 3 equiv. B_2cat_2 heated to 80 ºC for 48 hours (500 MHz; d_5-pyridine; 298 K; $SiMe_4$). A mixture of **1**, **3** and **4** is still observed, however the quantity of **4** is significantly greater than after 24 hours.

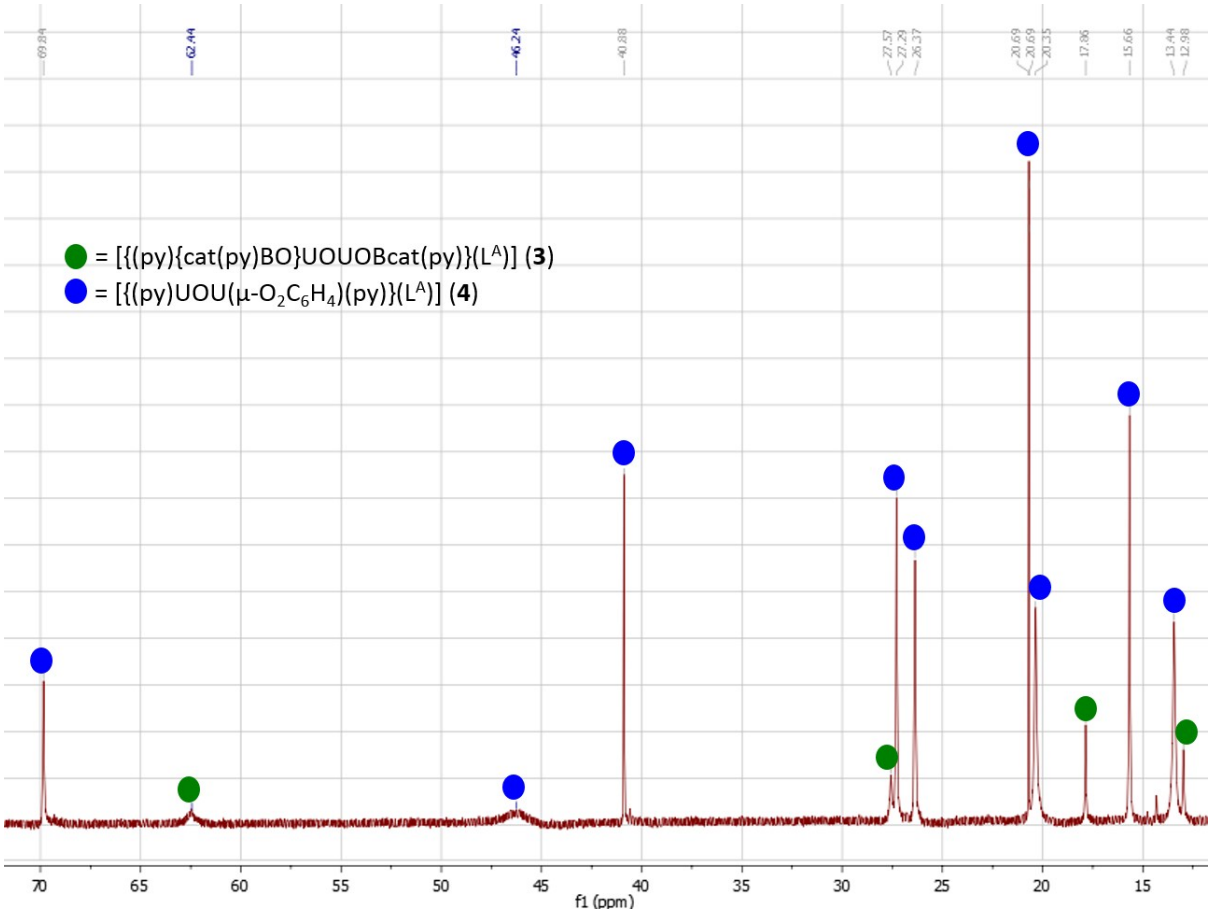

Figure S34. Expanded view of the ^{1}H NMR spectrum of **1** + 3 equiv. B_2cat_2 heated to 80 ºC for 48 hours (500 MHz; d_5-pyridine; 298 K; $SiMe_4$). A mixture of **1**, **3** and **4** is observed.

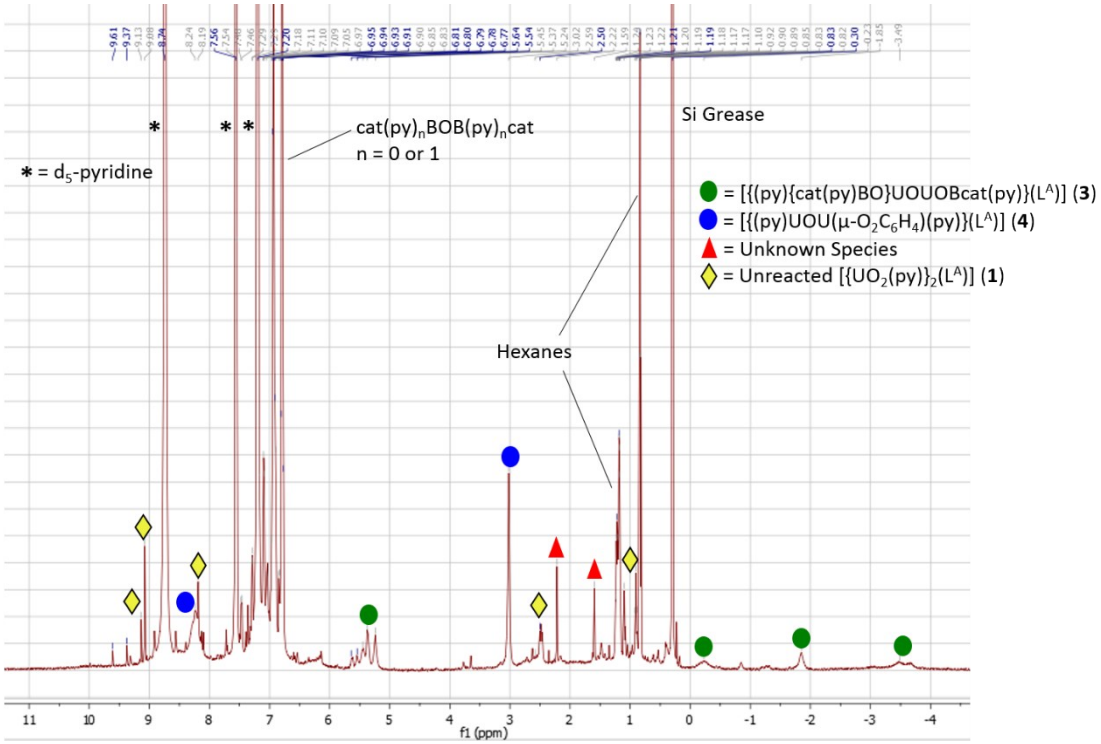

Figure S35. Expanded view of the ^{1}H NMR spectrum of **1** + 3 equiv. B_2cat_2 heated to 80 ºC for 48 hours (500 MHz; d_5-pyridine; 298 K; $SiMe_4$). A mixture of **1**, **3** and **4** is observed.

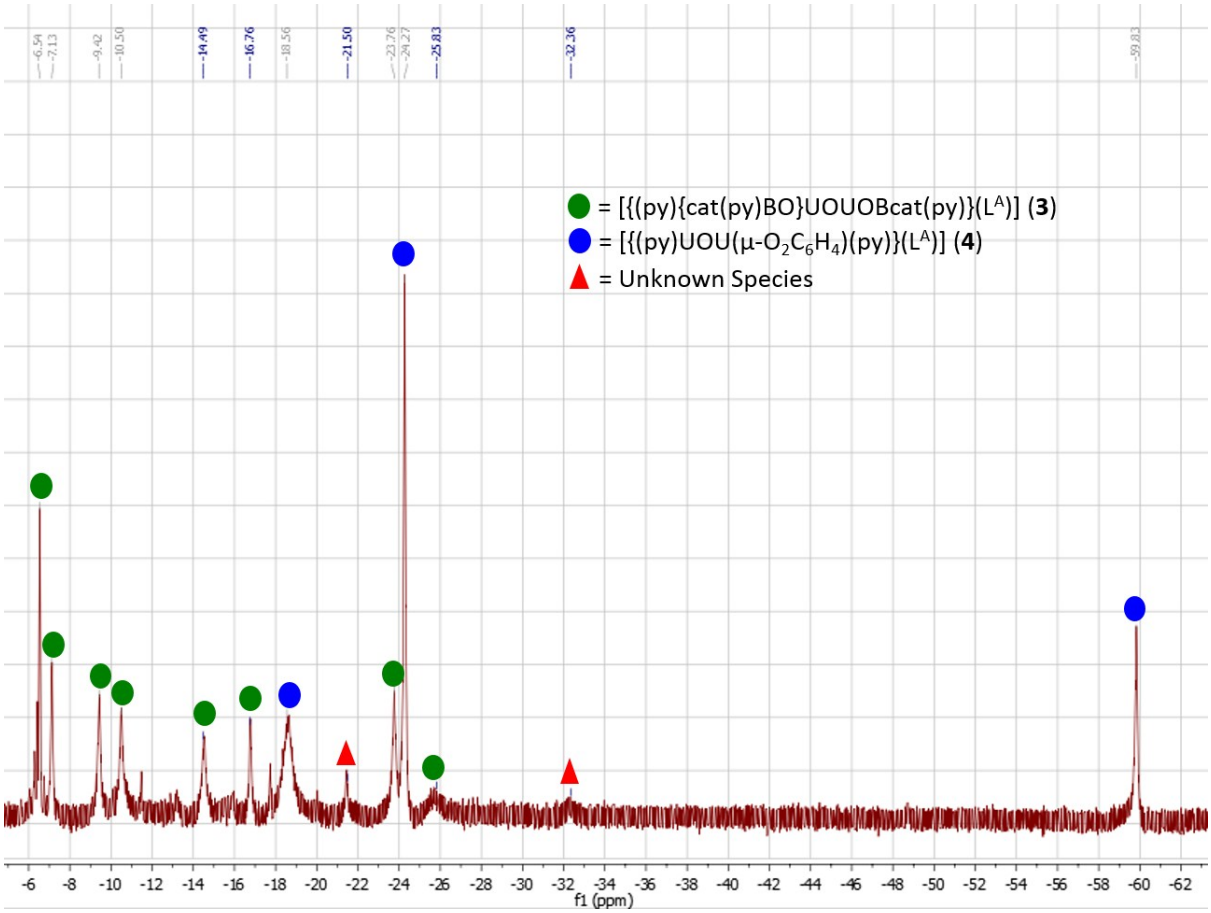

Figure S36. Expanded view of the ^{1}H NMR spectrum of **1** + 3 equiv. B_2cat_2 heated to 80 ºC for 48 hours (500 MHz; d_5-pyridine; 298 K; $SiMe_4$). A mixture of **1**, **3** and **4** is observed.

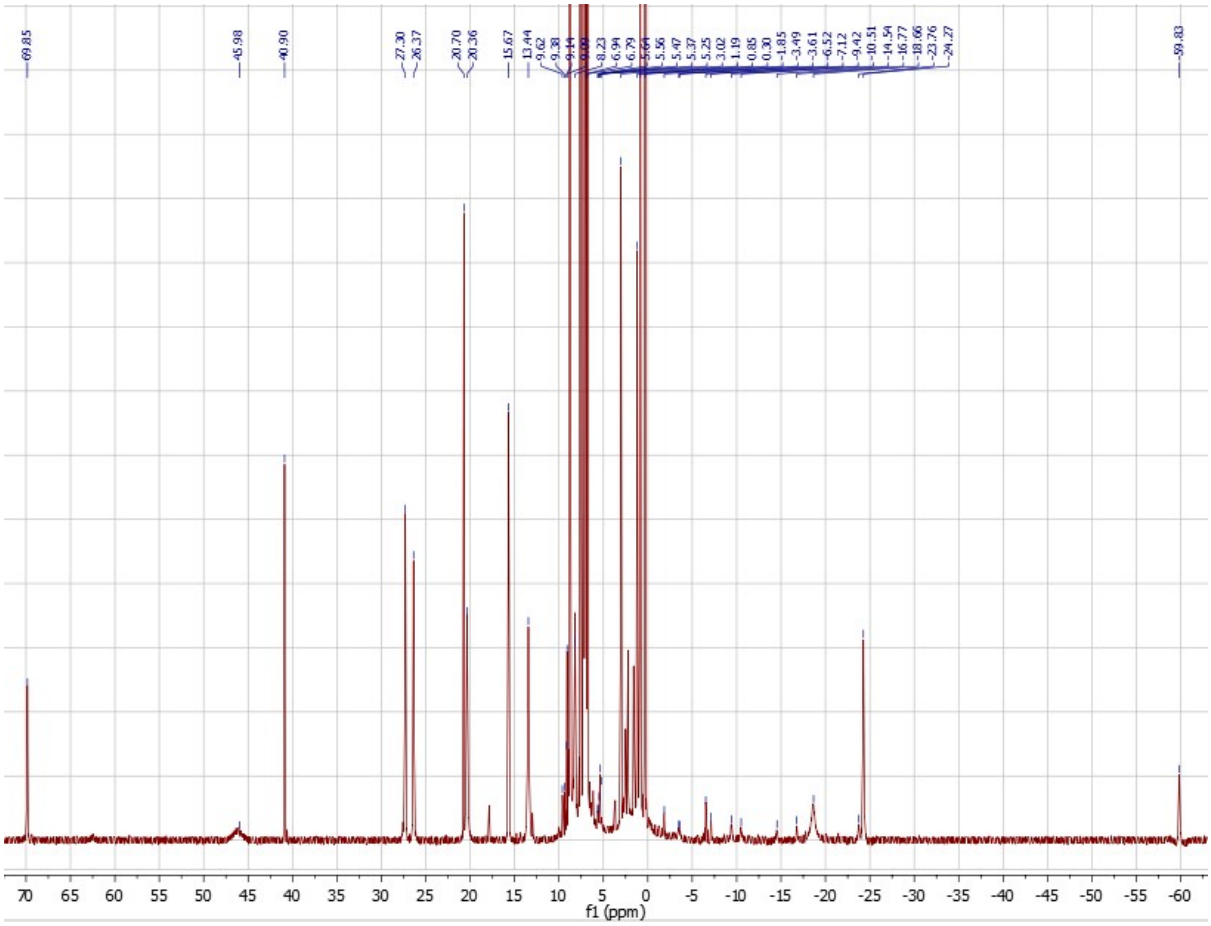

Figure S37. ^{1}H NMR spectrum of **1** + 3 equiv. B_2cat_2 heated to 80 ºC for 72 hours (500 MHz; d_5-pyridine; 298 K; $SiMe_4$). Complete consumption of **1**, and complete conversion of **3** to **4** is observed.

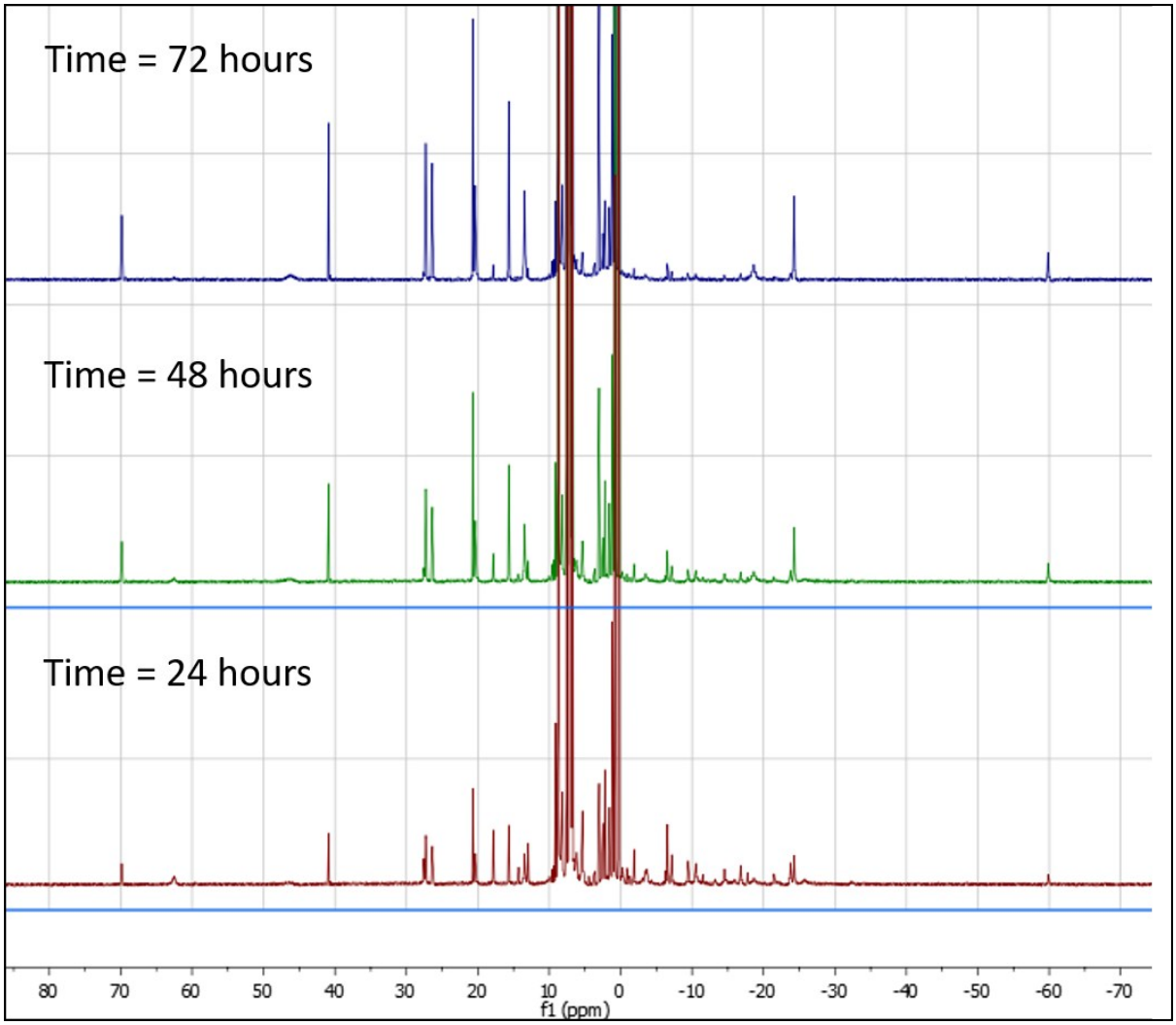

Figure S38. Stacked ^{1}H NMR spectra of **1** + 3 equiv. B_2cat_2 heated to 80 ºC for 24, 48 and 72 hours (500 MHz; d_5-pyridine; 298 K; $SiMe_4$).

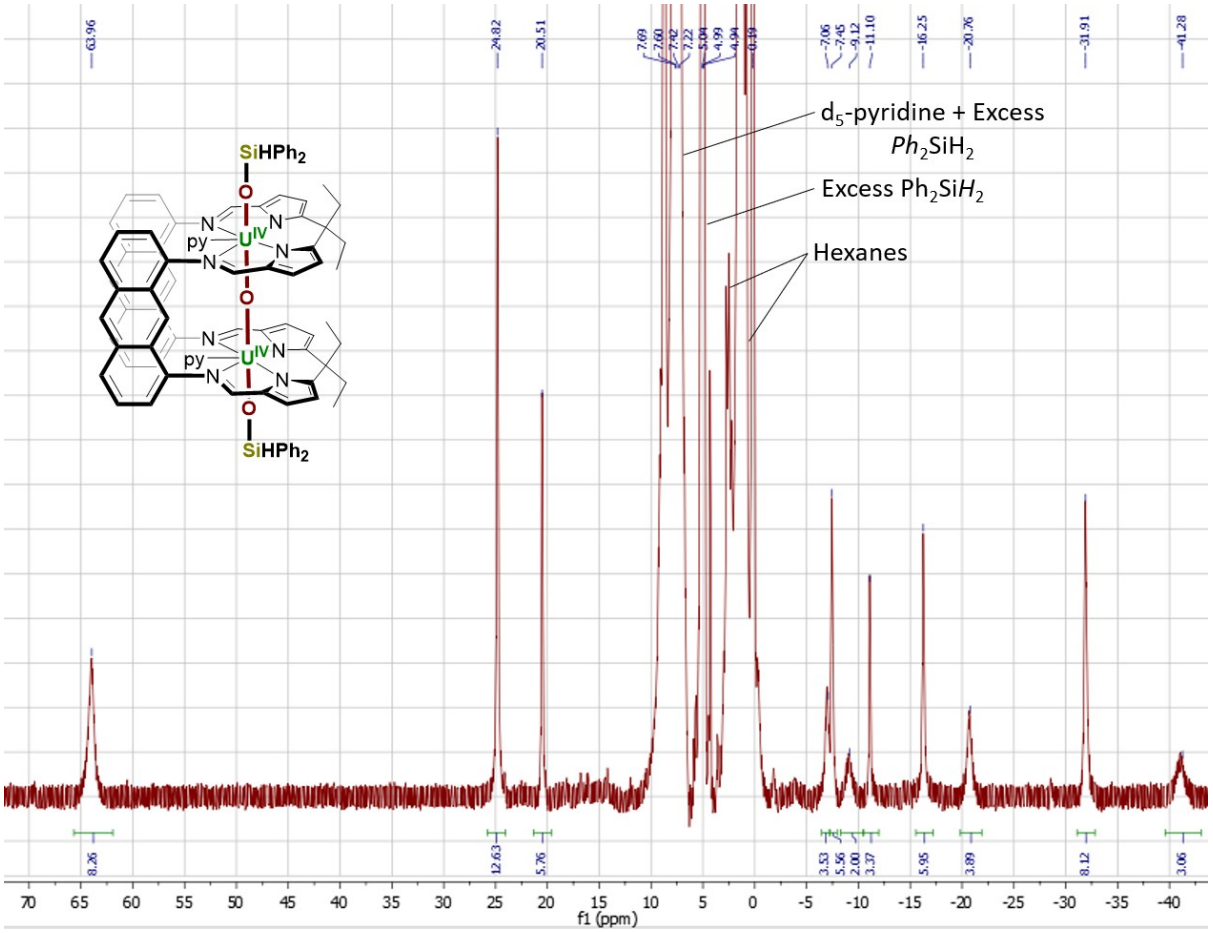

Figure S39. ^{1}H NMR spectrum of **5** generated *in-situ* (500 MHz; d_5-pyridine; 298 K; $SiMe_4$).

FTIR Spectra

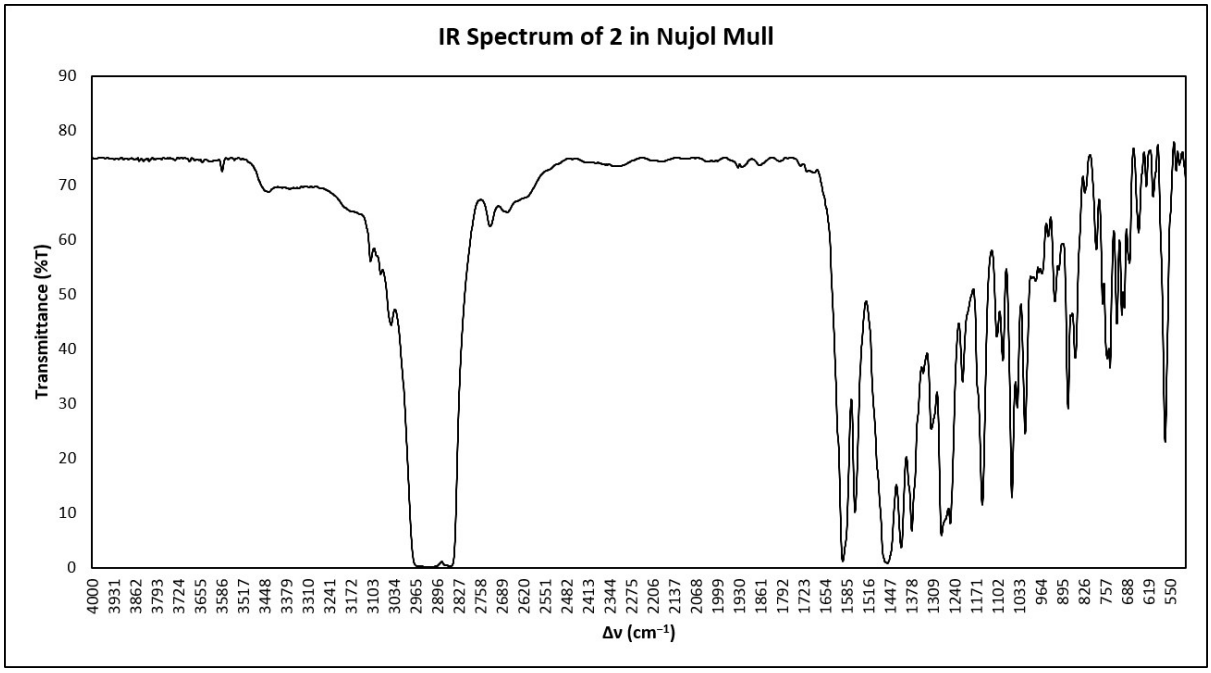

Figure S40. IR spectrum of **2** in nujol mull.

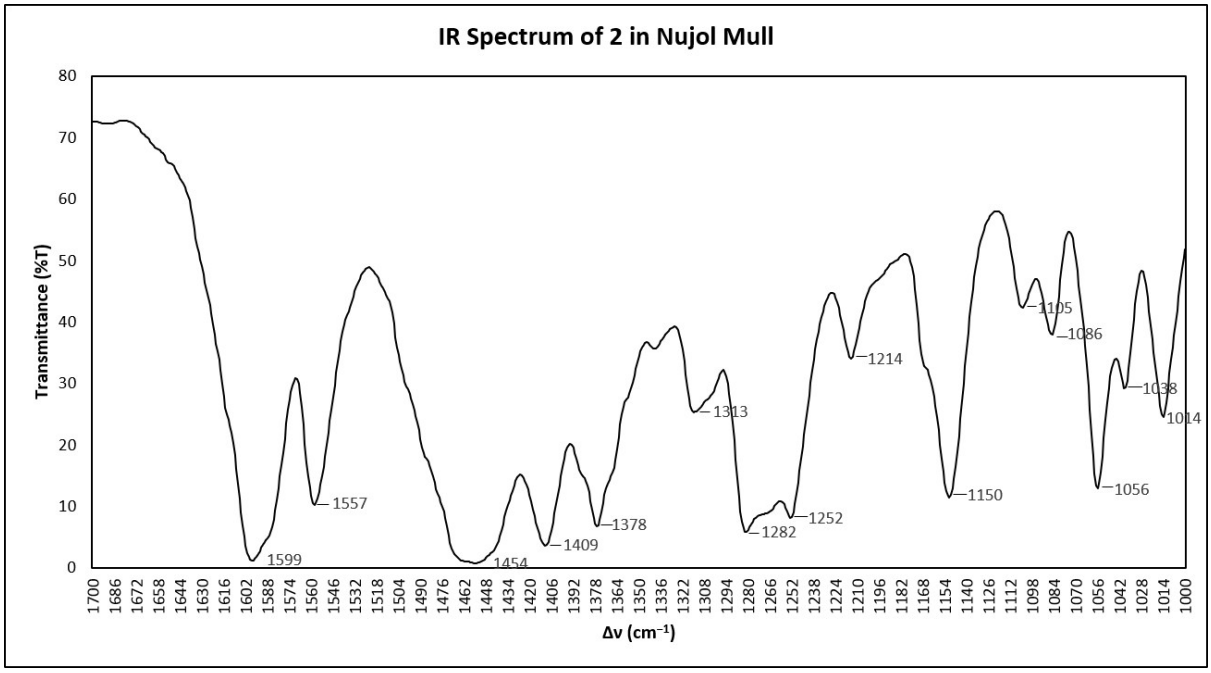

Figure S41. Expanded view of the IR spectrum of **2** in nujol mull.

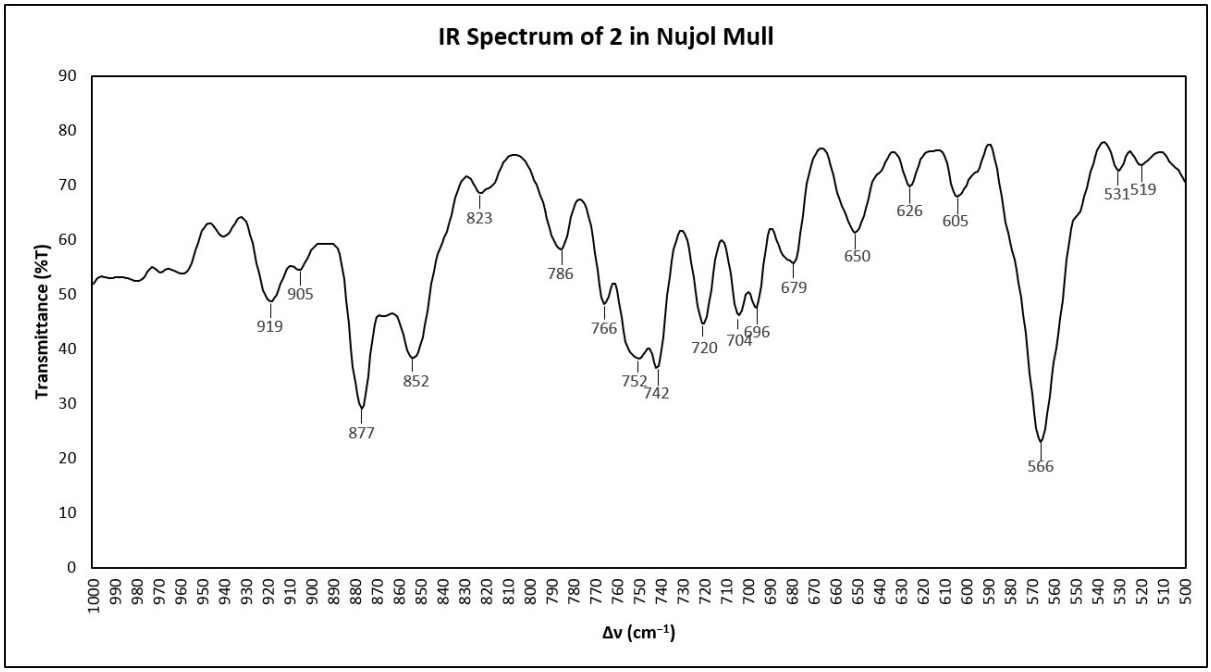

Figure S42. Expanded view of the IR spectrum of **2** in nujol mull.

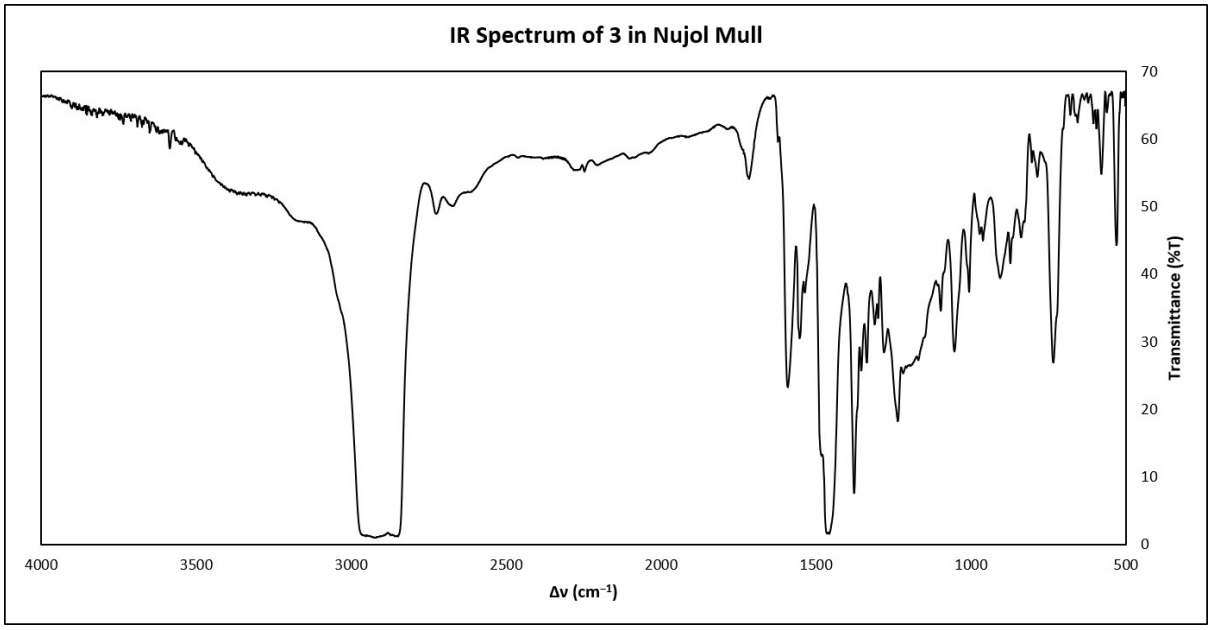

Figure S43. IR spectrum of **3** in nujol mull.

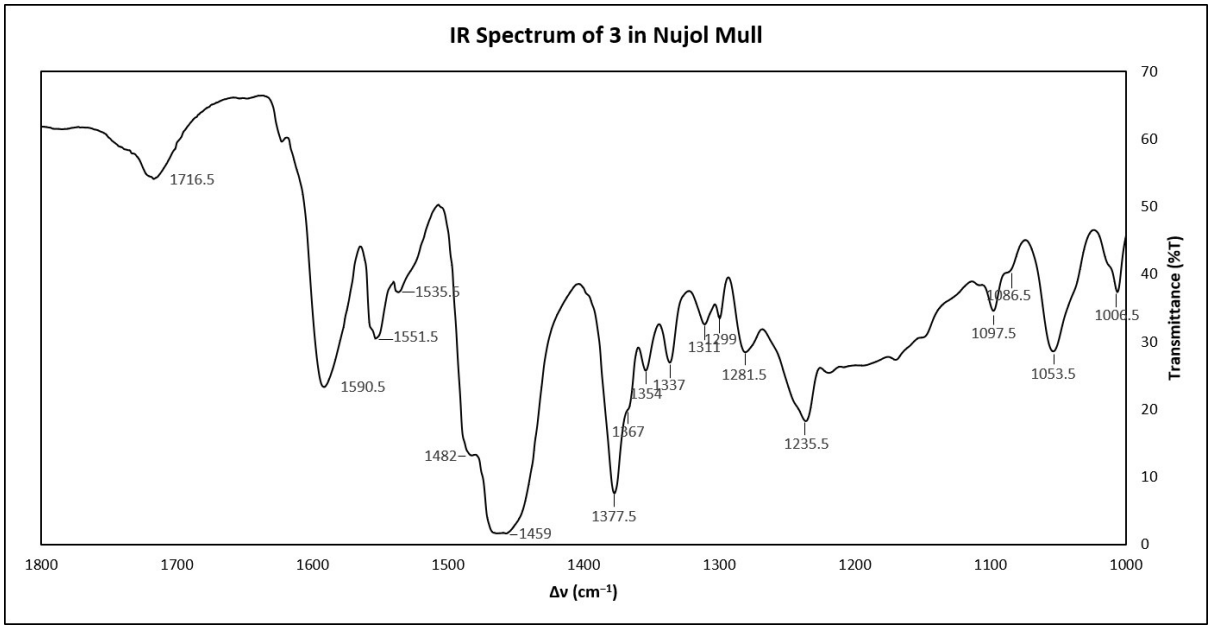

Figure S44. Expanded view of the IR spectrum of **3** in nujol mull.

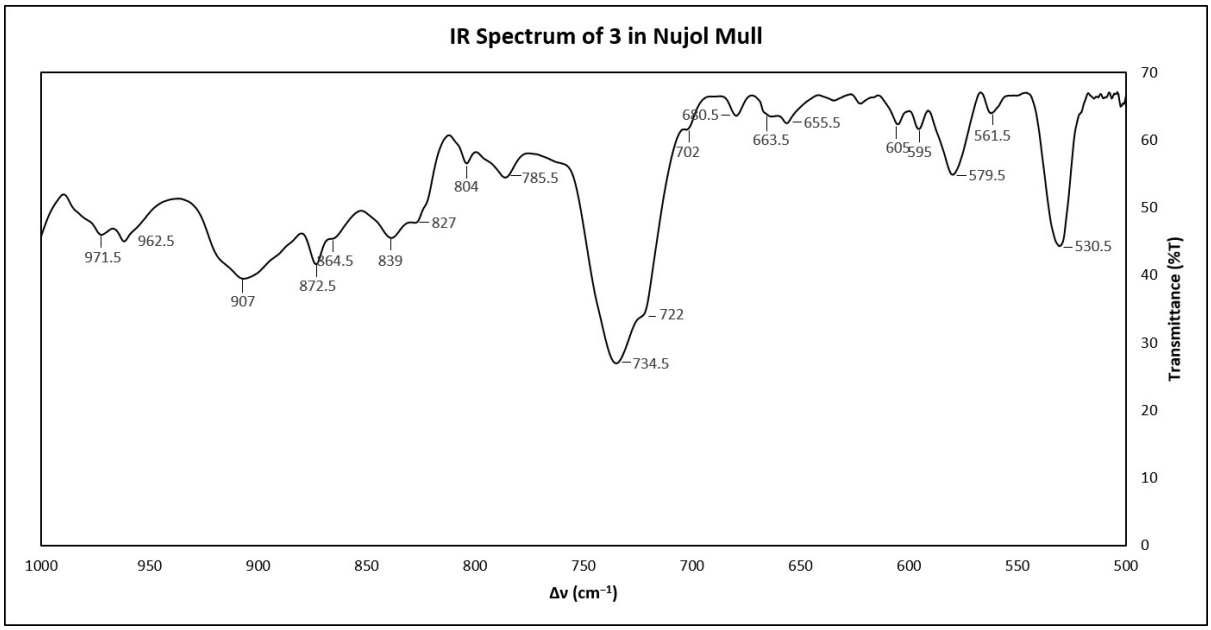

Figure S45. Expanded view of the IR spectrum of **3** in nujol mull.

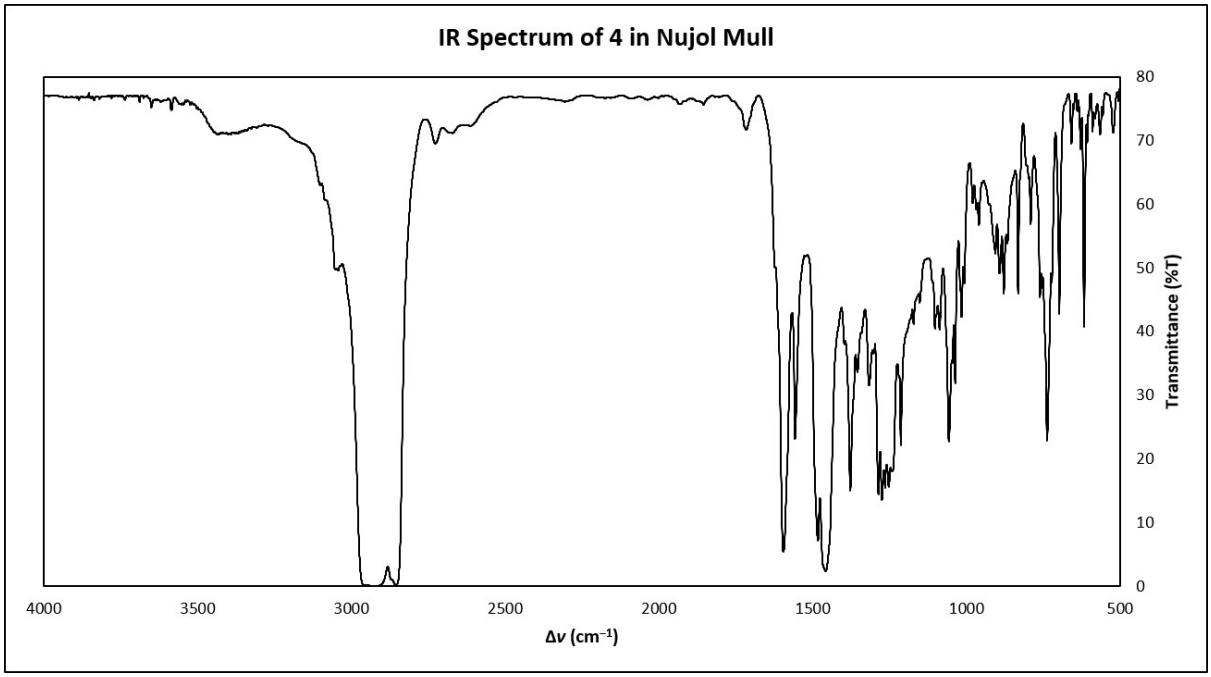

Figure S46. IR spectrum of **4** in nujol mull.

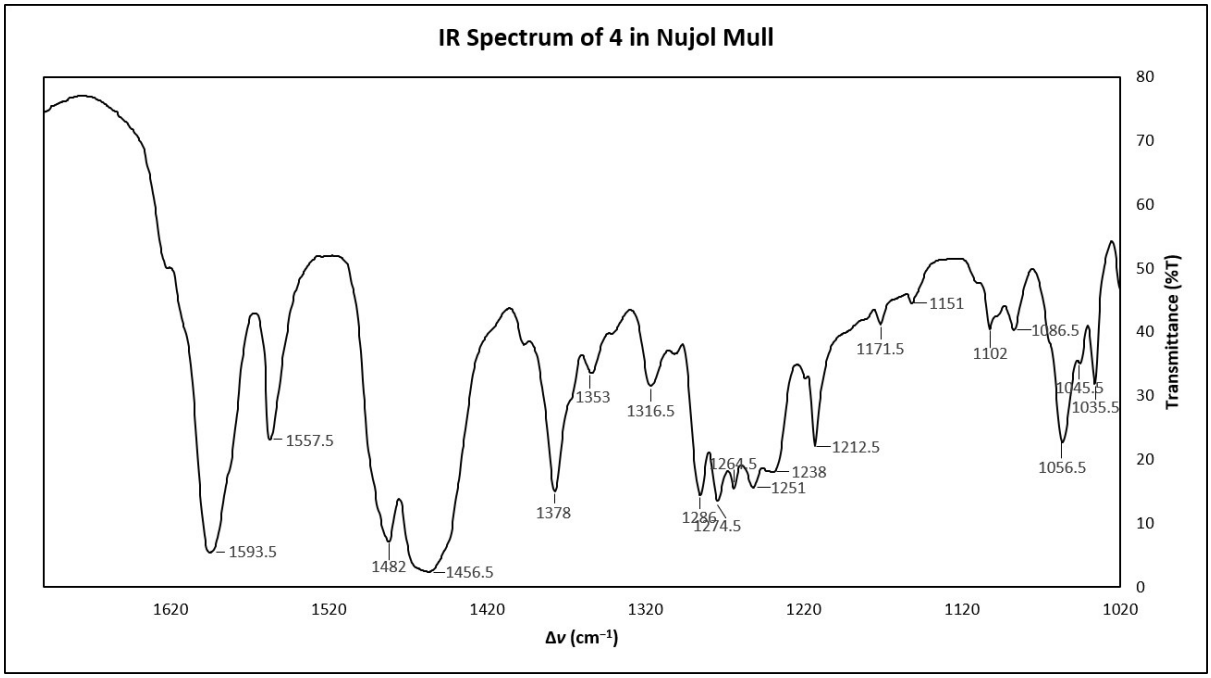

Figure S47. Expanded view of the IR spectrum of **4** in nujol mull.

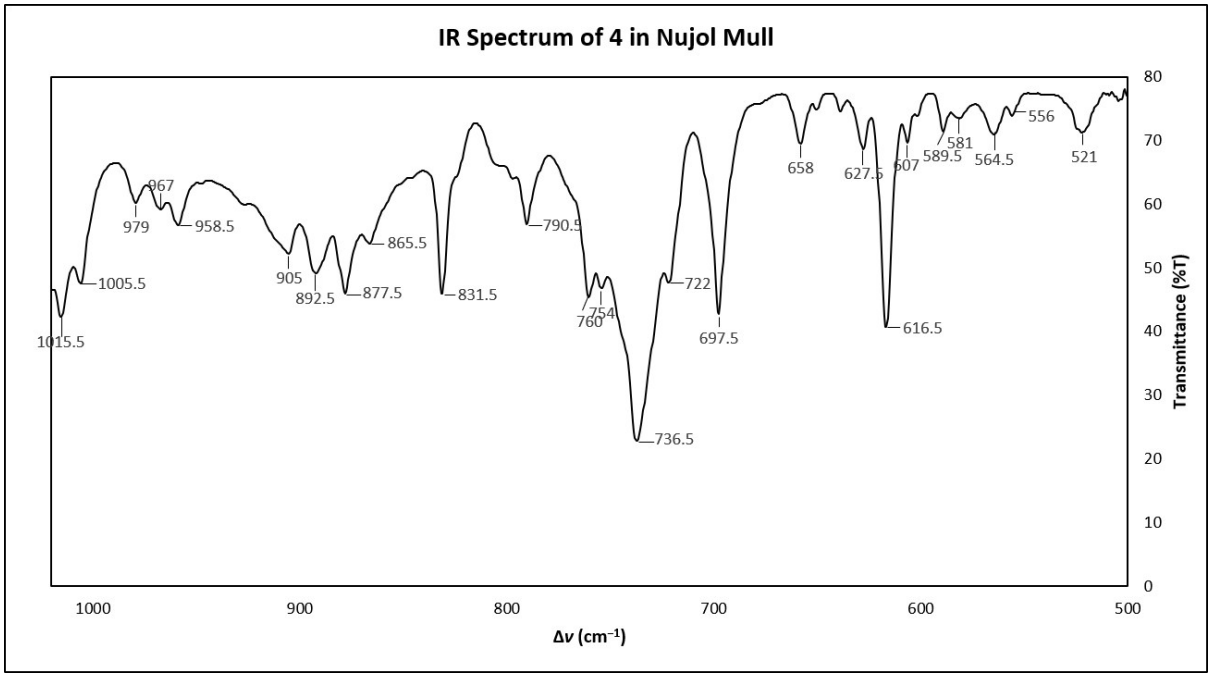

Figure S48. Expanded view of the IR spectrum of **4** in nujol mull.

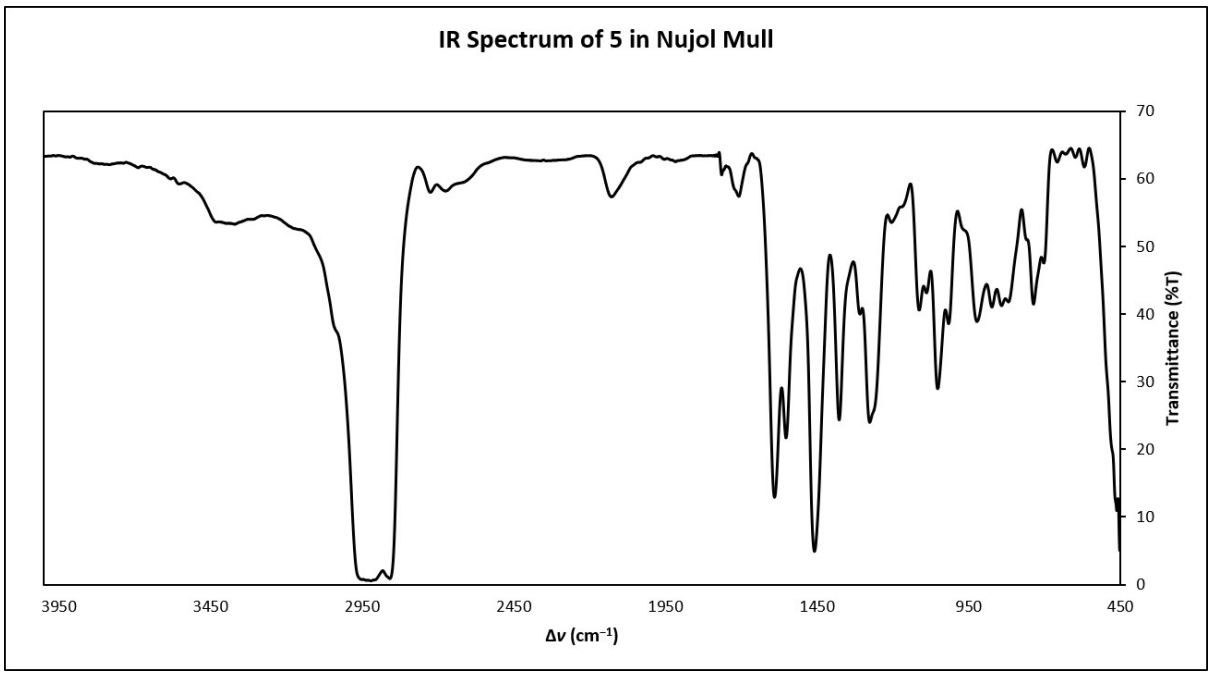

Figure S49. IR spectrum of **5** in nujol mull.

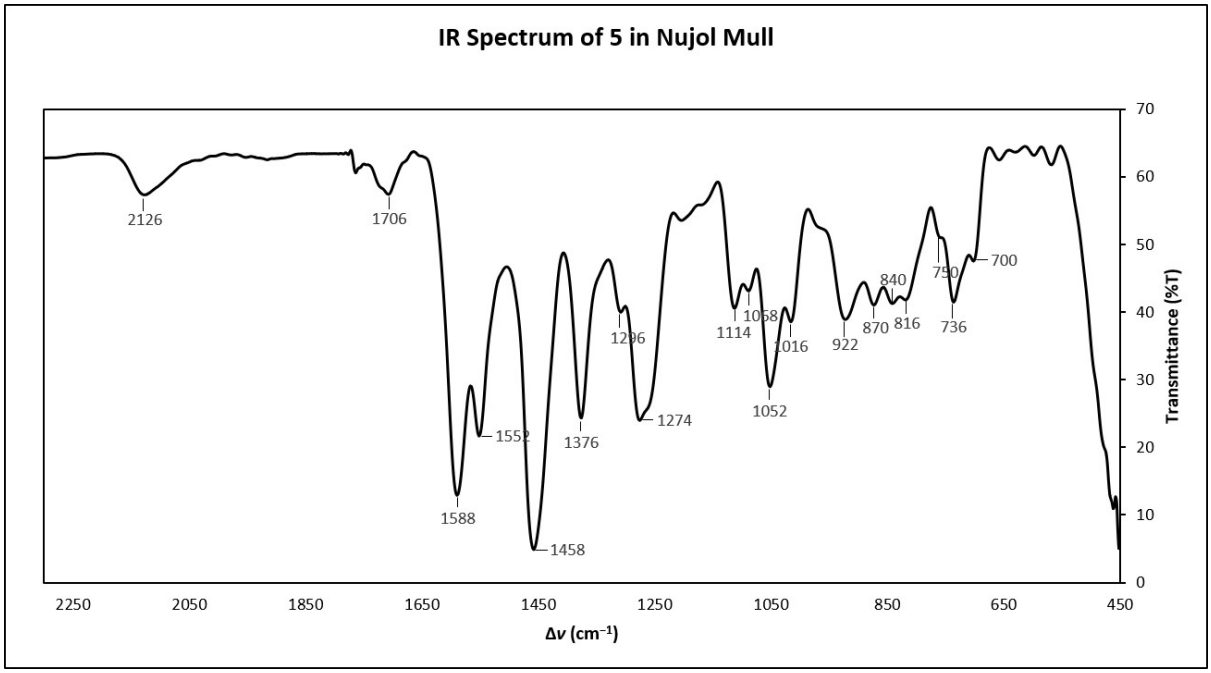

Figure S50. Expanded view of the IR spectrum of **5** in nujol mull.

References:

1. S. M. Mansell, B. F. Perandones, P. L. Arnold, *J. Organomet. Chem.* **2010**, *695*, 2814.
2. D. M. Barnhart, C. J. Burns, N. N. Sauer, J. G. Watkin, *Inorg. Chem.* **1995**, *34*, 4079.
3. E. Askarizadeh, A. M. J. Devoille, D. M. Boghaei, A. M. Z. Slawin, J. B. Love, *Inorg. Chem.* **2009**, *48*, 7491.
4. P. L. Arnold, G. M. Jones, Q-J. Pan, G. Schreckenbach, J. B. Love, *Dalton Trans.* **2012**, *41*, 6595.
5. G. M. Sheldrick, *Acta Cryst.* **2015**, *A71*, 3.
6. G. M. Sheldrick, *Acta Cryst.* **2015**, *C71*, 3.
7. O. V. Dolomanov, L. J. Bourhis, R. J. Gildea, J. A. Howard, H. Puschmann, *J. Appl. Crystallogr.* **2008**, *42*, 339.
8. A. L. Spek, *Acta Cryst.* **2015**, *C71*, 9.